Crude oil infiltration and movement in first-year sea ice: Impacts on ice-associated biota and physical constraints

Principal Investigator: R. Eric Collins[1]

Co-Investigators: Bodil Bluhm [2], Rolf Gradinger[2], Hajo Eicken[3]

Graduate Students: Kyle Dilliplaine[1], Marc Oggier[3]

[1] College of Fisheries and Ocean Sciences, University of Alaska Fairbanks

[2] Department of Arctic and Marine Biology, The Arctic University of Norway

[3] International Arctic Research Center, University of Alaska Fairbanks

FINAL REPORT

OCS Study BOEM 2017-087

December 2017

The views and conclusions contained in this document are those of the authors and should not be interpreted as representing the opinions or policies of the U.S. Government. Mention of trade names or commercial products does not constitute their endorsement by the U.S. Government.

TABLE OF CONTENTS

LIST OF FIGURES

LIST OF TABLES

ABSTRACT

The Arctic marine environment is facing increasing risks of oil spills due to growing maritime activities such as tourism and resource exploration. Entrainment and migration of oil through the sea ice brine channel system may pose a considerable risk to the biota that rely on the ice for food and shelter. These ice-associated biological communities are the base of an Arctic food chain that supports a hugely productive community of polar bears, birds, walruses, whales, and ultimately humans. To investigate the possible impacts of oil, we designed mesocosms allowing for the careful growth of artificial sea ice that would be reflective of natural sea ice. These mesocosms were inoculated with biological cultures collected from landfast sea ice near Utqiaġvik (formerly Barrow), AK. Once environmentally-similar ice conditions were established in the tanks, we evaluated the impact of Alaska North Slope crude oil on transplanted sea ice biota using two different oiling scenarios: discrete oil lenses and dispersed emulsions. We found that North Slope crude oil penetrated farther into overlying sea ice than observed in previous experiments (NORCOR, 1975, Glaeser and Vance, 1972, Dickens 2011). We also found that the presence of oil resulted in notable negative impacts on the biological community, with complete inhibition of ice algal growth. These findings suggest that an oil spill in ice-covered waters could have substantial and lasting negative impacts on the microorganisms at the base of this critical Arctic food chain.

INTRODUCTION

Background

Large unexploited oil reserves have been estimated to occur in the Arctic. The recent discovery of a 10-billion barrel reserve near Utqiaġvik, Alaska, reflects ongoing efforts to identify resources for exploitation in the region (Gautier et al. 2009). An observed declining trend in sea ice cover led Harsem et al. (2013) to predict that the Chukchi and Beaufort Seas will have an additional three ice-free months per year by 2040. Improved accessibility due to reduced ice cover could support increased shipping and oil and gas exploration and extraction activities (Arctic Council 2009).

Despite the expectation of an "ice-free" summer (<1-million km^2) within 50 years, sea ice will continue to form during the Arctic winter each year (Overland and Wang 2013). Landfast sea ice occurs annually along coastal northern Alaska for nine months, and pack ice can drift inshore even during the summer ice-free period (Mahoney et al. 2007). The presence of sea ice is a hazard to the marine shipping and petroleum industries and an obstruction to oil spill responders. Recent Arctic research has focused on detection of spilled oil in ice (Bassett et al. 2016), the interaction and distribution of oil with and within the porous sea ice medium (Petrich et al. 2013), and cleanup techniques and technology (Buist et al. 2011).

Sea ice geophysics and oil

Oil spilled under sea ice, as might occur from a well blowout or damaged vessel, will rise through the water column and pool at the underside of the ice, accumulating in recessed undulations (Glaeser and Vance 1972; NORCOR 1975; Figure 1). Oil spilled in open Arctic waters can also find its way under the ice as leads close and force the oil downward (MacNeill and Goodman 1987). Ice in dominantly thermodynamic growth, as occurs in calm weather conditions, can encapsulate the oil within days (NORCOR 1975; Buist and Dickins 1987; Fingas and Hollebone, 2003; Karlsson 2009). Oil released underneath ice with a porosity $\geq$ 15% quickly saturates the skeletal layer and ice, and oil has been observed to infiltrate sea ice with porosity as low as 10% (Karlsson et al. 2011; Otsuka et al. 2004). It is generally assumed that oil penetration depth in ice ranges from 0.1–0.25 m, increasing with warmer seasonal temperatures (Petrich et al. 2013). Encapsulated oil is thought to remain trapped until spring warming increases porosity, allowing migration of oil to the surface, or under-ice ablation remobilizes the oil under the ice (NORCOR 1975). Oil migrates farther into the ice cover as the interconnectivity and the brine volume fraction increase during the spring melt. As the ice deteriorates, oil occupies the interstices within and between the ice crystals (Martin 1979; NORCOR 1975; Wolfe and Hoult 1974). In saturated ice, oil can weigh 4.5–7 % wt of the sea ice mass (Karlsson et al. 2011; Otsuka et al. 2004).
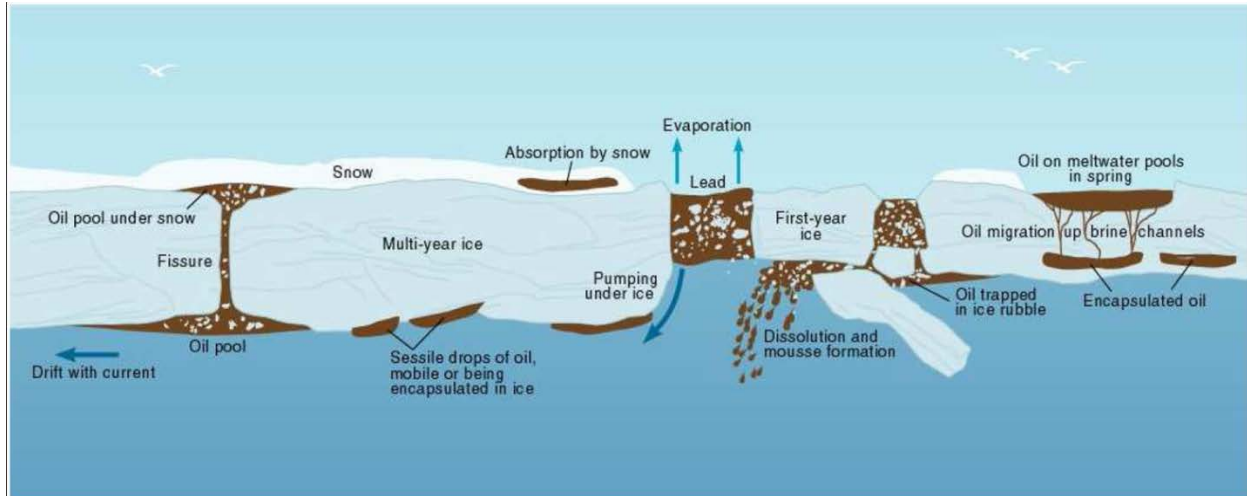
Figure 1. Oil interactions with sea ice (Reprinted from AMAP 2010).

Although sea ice porosity is relevant to oil movement, entrainment and migration are more likely to be controlled by other parameters including oil thickness, pore space geometry (e.g., pore size, presence of throats/necks), and macroscale sea ice process (e.g., desalination, brine convection) (Dickins 1992). Recent experimental studies have focused on the microscale interaction between oil and sea ice to determine what governs the migration process (e.g., Dickins 2011; Maus et al. 2013; Salomon et al. 2016). Additionally, simulation studies of brine displacement demonstrated that buoyancy forces (due to oil/brine density difference) are sufficient to overcome the capillary forces within a brine channel and to drive the oil upward (Maus et al. 2015).

Oil can be naturally emulsified (dispersed) in the upper water column under turbulent weather conditions or high current velocities (Tkalich and Chan 2002). The breakup of oil into small droplets can increase the amount of hydrocarbons dissolved in the water, a factor directly related to toxicity (Gardiner et al. 2013; Özhan et al. 2014). The size of dispersed oil droplets is tied to the degree of external energy operating on the oil (i.e., more energy creates smaller droplets) (Li and Garrett 1998), and the dispersed oil may affect biota differently than oil present in other forms, such as an oil lens.

Sea ice biology and oil

The Arctic sea-ice cover is host to a diverse biological community that includes bacteria, algae, and metazoan meiofauna (Gradinger and Zhang 1997; Gradinger et al. 1999). Occupying a brine channel system that extends throughout the ice, these organisms can grow to abundance and biomass concentrations 1–3 orders of magnitude greater than found in the underlying water column at certain times of the year (Figure 2; Lee et al. 2008; Manes and Gradinger 2009). On an annual basis, primary production in sea ice contributes 3 to >50% of total annual production in the Arctic (Gosselin et al. 1997) and provides a food source for pelagic and benthic fauna (Michel et al. 2006; Boetius et al. 2013). Ice algal blooms are a particularly important food source in early spring because they support zooplankton until the onset of phytoplankton blooms

(Søreide et al. 2010). Sea ice communities are ecologically sensitive because numerous zooplankton and larval stages of animals depend on sea ice algae for growth, which in turn passes into higher trophic levels like birds, walrus, and whales.

Figure 2. Algal community in the skeletal layer of sea ice near Point Barrow, Alaska.

Little research exists examining the biological consequences of under-ice oil spills, and there remains a need to better understand the possible impacts to the inhabitants of this important ecosystem. In an industry-funded project in the 1980's, an experimental oil spill under nearshore landfast ice close to Baffin Island caused strong declines in ice copepods and polychaetes (Cross and Martin 1987), while no strong effect was observed on primary productivity of ice algae sampled near (but not within) the spill (Cross 1987). Decker and Fleeger (1984) found that oil pollution caused delays in colonization and reduced abundances of benthic polychaetes but observed lesser effects for nematodes. In a comparison of Arctic and sub-Arctic zooplankton, *Calanus finmarchicus* showed a stronger negative response to exposure to the polycyclic aromatic hydrocarbon (PAH) pyrene than did *Calanus glacialis* (Hjorth and Nielsen 2011). Despite these studies, very little is known about the response of sea ice organisms to oil exposure, particularly within the ice matrix, or the consequences of the complex interactions of oil, ice, and biology.

The high concentration of sea ice biota at the ice/ocean interface leaves the community particularly vulnerable to oil exposure from below. Oil exposure to sea ice has been shown to inhibit ice algal growth (Brakstad and Nonstad 2008) and decrease meiofaunal abundance (Cross and Martin 1987a); however, the response of ice algae and phytoplankton to oil exposure varies markedly between Arctic studies. Siron et al. (1993) released oil under sea ice with continuous dilution of the water column and noted inhibition of phytoplankton growth but no discernable change in the community composition. Cross (1987) noted no change in ice algal composition, cell density, biomass, or productivity after light oil-dosing under ice near (but not within) an oil spill. Fiala and Delille (1999) found inhibited biomass accumulation in sea ice algae dosed with crude oil *in situ*.

Biological impacts from oil exposure are difficult to predict because there are species-specific responses within each group of organisms (e.g., algae, bacteria, etc.). For example, depending on the concentration, the source oil, and the species, phytoplankton can be either inhibited or stimulated by crude oil exposure (Hsiao 1978; Özhan et al. 2014). Varying species-specific responses can result in community composition shifts within the algal, bacterial, and benthic meiofauna (Gerdes et al. 2005; Gilde and Pinckney 2012; Elarbaoui et al. 2015).

There are a few studies of the microbial community responses to oil contamination of sea ice, and there remains a need for better understanding of the potential for biodegradation in that environment. Several studies report a stimulation of the bacterial community by the addition of oil. Atlas et al. (1978) released oil under ice in May and incubated it for three weeks; degradation rates appeared to be slow but were not quantified. Oil spill mitigation through biodegradation processes depends on a shift in relative abundance of oil-degrading bacteria in the presence of oil. Bragg et al. (1994) showed that nutrient additions promoted bacterial growth and enhanced the degradation rate.

Overall, few studies have quantified biological effects of oil on sea ice biota and even fewer have studied effects on phototrophs and heterotrophs in the same study. While research is needed to discern the responses of ice biota, *in situ* experiments are constrained by variable and patchy ice conditions and environmental regulation. This study provided a framework for conducting oil exposure experiments under simulated *in situ* conditions.

Study Objectives

The primary goals of this study were to investigate

1. rates and mechanisms of crude oil infiltration and movement in sea ice on the microscale; and
2. effects of oil on ice-inhabiting biota in Alaskan coastal landfast ice.

A secondary goal was to investigate the impact of ice biota on the oil intrusion process, which has not previously been documented. The study was designed to combine relevant field measurements of geophysical and biological properties of Alaska landfast ice with laboratory experiments focused on sea ice porosity and oil migration.

The specific objectives to address the project goals included

1. growing sea ice in mesocosms using artificial seawater under controlled laboratory conditions;
2. analyzing changes in sea ice flora and faunal composition in association with exposure to oil within the mesocosms;
3. assessing the toxicity of oil on sea ice meiofauna; and
4. adapting and applying qualitative and analytical models to the small-scale movement of oil in ice.

This report provides results of *in situ* experiments to evaluate the response of algal biomass, extracellular polymeric substances (EPS), and algal and bacterial abundance to two oil release scenarios: calm release with oil lens formation and physical dispersion in which oil was mechanically emulsified.

It was predicted that algal biomass, EPS, and algal and bacterial abundance would all decrease in tanks exposed to oil, with greater declines in the physically dispersed treatment. This report provides details on the design of the laboratory mesocosms, which successfully grew sea ice similar to first-year landfast sea ice. Toxicity assays are only briefly discussed because they were hampered by low meiofaunal survival. Finally, we present detailed geophysical measurements related to the structure of the ice and the migration of oil.

METHODS

Overview

The design, preparation, and execution of the experiments consisted of three parts:

1. Designing mesocosms to conduct oil in ice experiments

2. Collecting natural sea ice communities from fast ice close to Utqiaġvik, Alaska, as seed for the experiments

3. Conducting the experiments in the mesocosm tanks

Experimental oil releases under artificial sea ice were conducted in 2014 (Y1) and 2015 (Y2). Outcomes from Y1 were used to improve the design for Y2. Initial tank designs were based on Karlsson (2009). Six individual tanks were used during experiments to investigate three treatments (each with two replicates) per year. In Y1, treatments consisted of biological control (no oil) and oil lens treatments (with and without biota). Y2 treatments included a control, oil lens with biota, and a physical emulsification (with biota) used to test effects of low volumes of oil representative of a mechanical dispersion process (i.e., wave action or turbulent well-head release).

In both years, the artificial sea ice was seeded with biota (bacteria and algae) collected from fast ice in Utqiaġvik, Alaska. This field sampling was also used to determine basic biological parameters in natural landfast sea ice for later comparison with the tank biota. Biological samples and physical characterization cores were collected prior to oil release and on the final day of the experiments.

Tank Design

Six High-Density Polyethylene (HDPE) square tanks (0.6 x 0.6 m sides, 1 m tall) were constructed (see Figure 3) in a cold room laboratory so temperature could be adjusted to control ice growth. Each tank held 360 L of artificial seawater made from Instant Ocean aquarium salts. Frazil ice was simulated using hoarfrost crystals collected from the surface of lake ice; a 3 cm thick layer was added to the tanks when the water reached the freezing point (-1.8°C). The target growth rate for ice was 1 cm day^{-1}. Ice thickness was monitored using in-tank thermistor chains and monitoring ice temperature profiles.

Slight modifications were made to the tanks in Y2 to get more consistent ice growth. The cold room was held at a constant temperature of -15°C and the mean seawater salinity before freezing was lowered to 26 PSU. The variable speed controllers used in Y1 for heater control were replaced with three 10 watt and one 15 watt heaters per tank. Heaters were turned on or off to control ice growth. Frazil ice was simulated using clean crushed freshwater ice, resulting in larger surface ice crystals (~1 mm) in Y2.

Figure 3. Incubation tanks (left) and schematic showing positions of sensors and equipment in each tank (right): (A) LED light fixture, (B) datalogger, (C) thermistor chain, (D) temperature and salinity probe, (E) 4π light sensor, (F) circulation pump, (G) heater, and (H) pressure release bladder.

Field Sampling

Field sampling of natural landfast ice communities and characterization of the *in situ* environmental conditions occurred in April 2014 (Y1) and March 2015 (Y2). Sampling occurred on level landfast ice close to Utqiaġvik, Alaska. Landfast sea ice was collected using a Kovacs Mark II 9 cm diameter ice corer. Ice temperature was measured in a single core at 10 cm intervals immediately after coring. Salinity samples were collected from an adjacent core by sectioning and melting 5 cm intervals for direct measurement with a salinity probe.

Irradiance was simultaneously measured at the ice-air interface and 10 cm below the ice-water interface with light sensors. The bottom 10 cm of ice was sampled in three replicate cores for quantification of chlorophyll *a* concentration (Chl *a*), EPS concentration, and bacterial abundance. The 10 cm bottom portion of each ice core was divided into two horizons, 0–2 and 2–10 cm, with 0 representing the ice-water interface. Sections were melted at 4°C. Cores were melted in the dark and with the addition of 100 ml of 0.2 µm-Filtered Sea Water (FSW) per cm of core to prevent osmotic shock to the ice biota (Garrisson and Buck 1989). Sections were processed once entirely melted (i.e., after 3–30 hours).

A custom-built carbon fiber ice corer (Jon's Machine Shop, Fairbanks, Alaska; 20 cm inner diameter) was designed to collect a large volume of ice for tank inoculation. A total of 75 ice cores were collected and the bottom 1–3 cm of each core, which typically contains most of the biomass in Alaska landfast ice (Gradinger et al. 2009), was removed and melted with the addition of FSW. Pooled sections were initially held in an incubator in Utqiaġvik under low light, approximately 20 µmol photons m-2 s-1 at 1°C. The inoculum was transported to Fairbanks, Alaska where it was held at 1°C with a salinity of 28 under constant light conditions, 20 µE m-2 s-1 with aeration, until use within the tanks. No supplemental light was provided during the approximately six hour transport from Utqiaġvik to Fairbanks.

In Y2, bottom ice for biological analyses was divided into three sections, 0–2, 2–5, and 5–10 cm (0=ice-air interface) to improve vertical resolution. A total of 64 ice cores were collected for inoculation, as described above.

Experimental Design

In Y1, six tanks were randomly assigned to one of three treatments, each with two replicates. Treatments included Biological Control with biota but without oil (BCY1; Biota+, Oil-), Oil Lens without biota (LY1; Biota-, Oil+) and Oil Lens with biota (BLY1; Biota+, Oil+) (Figure 4a). After the biological inoculation, ice was grown slowly for ten days to an average thickness of 18.6 $\pm$ 1.3 cm to allow for the establishment of a biological ice community. The time of Oil Release (OR) was used as the primary reference point for the experiment timelines. An initial coring was conducted two days prior to OR (OR-2) to obtain baseline values for parameters (e.g., Chl a, bacterial abundance, etc.) measured within each tank. Two days after baseline sampling, oil was released into the LY1 and BLY1 tanks. Three days after OR (OR+3), the BCY1 tanks were once again cored; LY1 and BLY1 tanks were excluded to limit oil contamination of the ice surface. Tanks were allowed to continue growing ice until thirteen days after OR (OR+13) when a final ice coring was conducted to determine the oil impact to the biological community.

The Y2 treatments (Figure 4b) included Biological Control with biota but without oil (BCY2; Biota+, Oil-), Emulsified Oil with biota (EOY2, Biota+, Oil+) to examine effects of lower oil concentrations, and Oil Lens with biota (BLY2) with a lower volume of released oil than in the similar Y1 treatment. Based on low Chl a concentrations observed in Y1, ice in Y2 was allowed to grow an additional day (eleven days) after biological inoculation to provide more time for biomass accumulation prior to OR. Final coring was completed ten days after OR (OR+10).
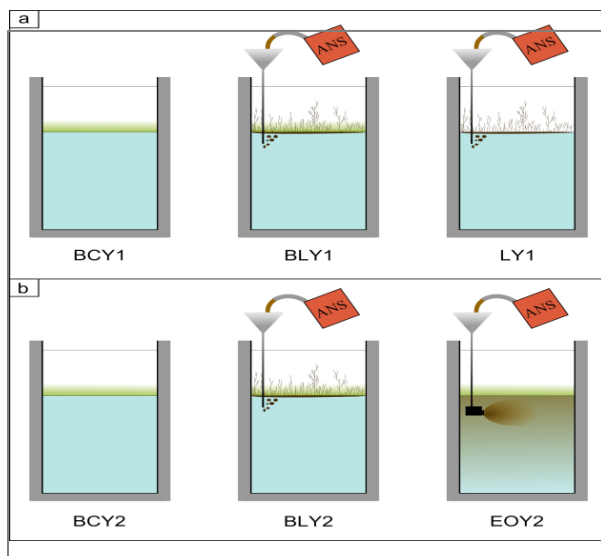

Figure 4. Treatment assignments tested in (a) Y1 (2014) and (b) Y2 (2015). ANS represents Alaska North Slope crude oil used for these experiments and green indicates biological inoculation.

Biological Inoculation

In Y1, 22 liters of inoculum were added to each of the six tanks. Ice was allowed to grow for 24 hours after inoculation to reduce osmotic stress to the released biota (Cox and Weeks 1975; Zhang et al. 1999) and to allow free movement of the organisms with the growing ice.

Results from Y1 indicated destructive freezing of biota into surface ice. Therefore, a different approach was used in Y2. Algae were cultured at UAF from environmental samples collected three months earlier and used to supplement the inoculations. Ice growth was initiated by adding crushed freshwater ice to the water surface. Ice was allowed to grow to an initial thickness of 10 cm. At that time, crushed freshwater ice was mixed with half of the inoculum to create a frazil ice slurry. Seven liters of algal culture were mixed with the environmental collections before being injected. After 24 hours, the remaining inoculum was released.

Oil Release

Alaska North Slope (ANS) crude oil was used for all experiments. The oil, collected from the Trans-Alaska Pipeline entry point, was provided by Alyeska Pipeline Services. Physical characteristics of the oil were determined in December of 2014 by SL Ross Environmental Research Ltd. ANS was cooled to a temperature of -2°C before addition to the tanks. In Y1, seven liters of oil were added to each of the lens treatment tanks, forming a 2 cm thick oil layer covering the entire ice bottom. As the oil was added, water was drawn from the bottom of the tank to maintain the water level. The core hole was plugged with a replacement ice core and sealed along its edges with freshwater to prevent oil percolation.

In Y2, two liters of oil were added to each lens treatment replicate using the same methods as Y1. For the oil emulsification treatments (EOY2), a small impeller was attached to the end of a syringe. The impeller was lowered underneath the ice and 500 ml of oil was injected into the impeller, which mechanically dispersed the oil below the ice.

Ice Core Sampling in the Experimental Tanks

All coring was done using a custom-built stainless steel corer (5 cm internal diameter) operated by an electrical drill. Six cores were randomly extracted from each tank during each coring event. Of those, two cores were used to measure salinity and oil volume, one core was used for ice microstructure analysis, and three cores were used for biological analyses. Cores were sectioned in order to provide a vertical distribution of each measurement. Immediately upon removal, salinity cores were cut into 2.5 cm sections, placed into airtight glass containers, and frozen at -20°C until further processing. Cores for other variables were sectioned to allow differentiation between bottom ice sections (ice-water interface), upper ice sections, and location of an oil lens (Figure 5).
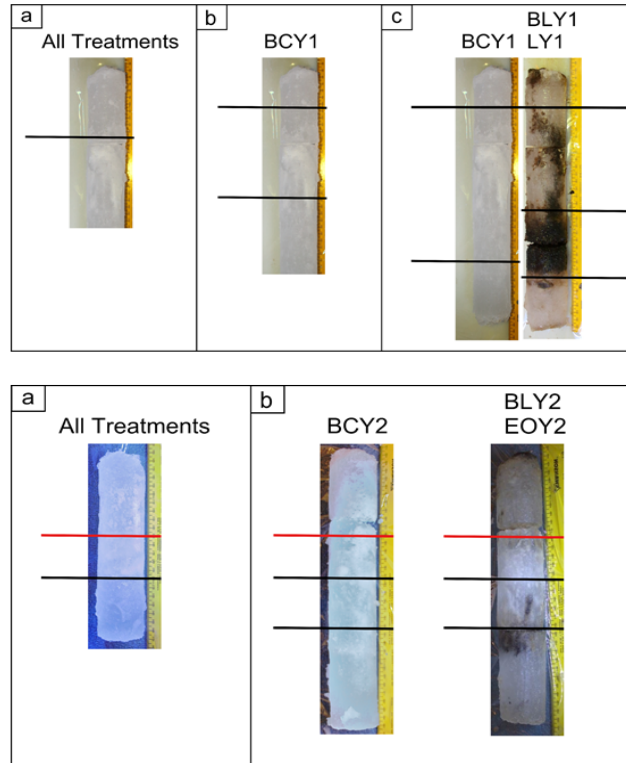
Figure 5. Schematic showing ice sectioning procedures. Lines represent where sections were cut. Ice above the red line was not included in the biological analyses. Y1 cores (top) were collected at (a) OR-2, (b) OR+3 in BCY1 only, and (c) OR+13. Y2 cores (bottom) were collected at (a) OR-2 and (b) OR+10.

Ice Core Measurements

Physical variables

Air, ice surface, water temperature, water salinity, and light measurements were recorded every 1 to 3 days. As ice thickness increased, adjustments to the surface irradiance were made by increasing LED light intensity to maintain an under-ice irradiance above the minimum threshold for ice algal growth (<1 µE m^{-2} s^{-1}) and similar to recorded environmental measurements (e.g., Cota and Smith 1991; Mock and Gradinger 1999). Three thermistor chains were placed in one randomly selected tank per treatment. Each chain had six thermistors evenly spaced at 5 cm throughout the ice and upper water layer. Salinity was measured in 2.5 cm sections and ice thickness was measured when cores were extracted. In Y2, ice blocks were also removed at the end of the experiment and frozen for post-processing of physical parameters. The blocks were used to supplement information on salinity and microstructure where a larger ice volume was required. For salinity and oil volume measurements, the core or block section was cut into horizontal segments after extraction and transferred to a sealed container for melting at room temperature. Samples with oil were poured in vertical graduated cylinders. Sealed cylinders sat overnight to allow oil droplets to settle at the surface. The oil lens thickness was measured along the glass and volume was estimated at the meniscus. Sea ice microstructure and oil inclusion and penetration were characterized using thin and thick section optical analysis. Observation of the

sections between crossed optical polarizers revealed ice crystals and detailed ice microstructure. Some samples were imaged with an X-ray tomographer (SkyScan 1074, Brucker Corporation, Billerica, MA, USA) to determine the amount of oil present within the sample using phase contrast techniques.

Biological variables

Ice sections were melted in the dark at 3℃ and processed as soon as they were completely melted (i.e., over a 72 hour period). Excess oil was removed from oiled samples by aspiration followed by adhesion to a glass funnel. Chl *a* concentration was determined in the melted samples by filtering 15-360 ml onto Whatman GF/F filters using vacuum filtration < 5 psi. Filters were extracted with 7 ml of 90% acetone at -20°C for 24 hours and samples were warmed to room temperature for 1 hour in the dark before fluorometric measurements were conducted using a TD-700 Turner Design fluorometer (Arar and Collins 1997). Fluorometer calibrations were conducted using pure Chl *a* standard (Sigma Aldrich).

Chl *a,* particulate organic matter (POM), and EPS samples were processed within three months of collection. Bacteria abundances were determined within five months of collection and within three weeks of filtration. Chl *a* concentration was determined fluorometrically using the method of Arar and Collins (1997). EPS concentrations were determined by the phenol/sulfuric acid method (DuBois et al. 1956; SOKI Wiki 2014). The equation of van der Merwe (2009) was used to convert µg Gluc eqv.L^{-1} ice (GEQV) to Xanthan Gum Equivalents (XGEQV) L^{-1} ice: µg XGEQV L^{-1} ice = 0.975 x µg GEQV L^{-1} ice + 0.879.

For bacterial enumeration, buffered formaldehyde was added as a preservative to each sample to a final concentration of 1%. Samples were stored in the dark at room temperature until later processing for enumeration by epifluorescence microscopy by DAPI staining (Porter and Feig 1980). Diatoms were counted as two groups, according to cellular fluorescent properties. Group 1 (intact) showed visible fluorescence of the plasma membrane and plastid and had no defined nucleus. Group 2 (damaged) showed weak or no plasma membrane or plastid fluorescence and had a well-defined nucleus. Diatom cell counts do not include empty frustules, which were enumerated and reported as proportional percent of frustule abundance (Frustules/Total Diatoms (excluding frustules)*100).

Toxicity Assays

Oil toxicity testing on sea ice meiofauna was conducted using a water accommodated fraction (WAF) prepared according to Singer et al. (2000). The 100% WAF solution was diluted with 0.2 µm filtered seawater to produce a dilution series at seven concentrations: 0, 6.25, 12.5, 25, 50, 75, and 100%. In Y2, a breaking wave WAF (BWWAF) was prepared according to Gardiner et al. (2013) to obtain higher *in situ* oil concentrations. Samples of the WAF and BWWAF were sent to TDI-Brooks International, Inc., for determination of hydrocarbon content. In Y1, the 100% stock solution of WAF had no measurable total petroleum hydrocarbons (TPH; combined aromatic and aliphatic hydrocarbons) and a total polycyclic aromatic hydrocarbons (TPAH)

concentration of 41.2 µg L^{-1}. In Y2, BWWAF TPH concentration was 5.32 mg L^{-1} and TPAH concentration was 285.6 µg L^{-1}.

In Y1, meiofauna (polychaete and nematode worms) were placed into triplicate glass jars with WAF at various dilutions from 0% to 100% with three replicates per dilution. Organisms were fed an algal culture at the initialization of the experiment and incubated in the dark at 1.5˚C for 7–12 days. Mortality was identified by gently prodding the organisms; an organism was considered dead after 60 seconds of no movement. In Y2, meiofauna (sea ice copepods, nematodes, and the acoel *Aphanastoma sp.)* were placed into triplicate plastic six-well plates with BWWAF at various dilutions from 0% to 100%. Organisms were fed and incubated for 12–13 days before testing for mortality as before.

Low initial populations (7–10 organisms per trial) and very high mortality rates in the control treatments (often upwards of 70%) yielded uninterpretable results in both years. Suggestions for improving future experiments are found in the Discussion.

Statistical analysis

All statistical analyses were conducted using R version 3.2.1. Linear Mixed Effects Regression models (LMER, R package lme4; Bates et al. 2014). Data using With/Without treatment as a factor were compared using one way ANOVA for each biological parameter (Chl *a*, diatom abundance, EPS, and bacterial abundance) for full cores and sections. LMER accounts for unequal sample size, the repeated measures design, and the random effect of the tank. Pairwise comparison of least-squares means was used for post-hoc assignment. A Welch's T-test was applied to the means of projected algal growth rates with actual concentrations. Simple linear regression models were used to correlate EPS with diatom and bacterial abundances, which were log transformed to meet normality requirements.

RESULTS

Fast Ice Observations in Utqiaġvik, Alaska

Physical variables

In Y1, level sea ice was selected for sampling within view (71.36675°N, 156.61715°W) of the Seasonal Ice Zone Observing Network (SIZONET; http://seaice.alaska.edu/gi/observatories) Barrow mass balance site. Snow depth ranged from 9 to 13 cm, and ice thickness varied between 134 and 138 cm (Table 1). Photosynthetically active radiation (PAR; light of 400–700 nm wavelengths available for photosynthesis) transmittance through snow and ice was 1.3% of the incoming radiation.

Table 1. Mean physical data measured during environmental collections from Utqiaġvik, Alaska, in Y1 (2014) and Y2 (2015).

	Y1	Y2
Air Temperature (°C)	-24.9	-19.0
Ice Thickness (cm)	136.0	127.0
Free Board (cm)	9.8	10.0
Snow Thickness (cm)	11.8	4.0
Water Depth (m)	8.4	7.3
Surface Irradiance (2π) μE m^{-2} s^{-1}	916	470
Under Ice Irradiance (4π) μE m^{-2} s^{-1}	11.4	8.4

In Y1, Ice temperatures showed a nearly linear increase from the ice surface (-14.3°C) to the ice bottom (-1.75°C; Figure 6, top left). Bulk salinity was highest in the surface and bottom segments of the ice, displaying the characteristic "C" profile of first-year ice before the onset of warming and melt (Figure 6, top right). Calculated brine salinity, based on ice temperatures, decreased from 172 at the top to 32 in bottom ice segments (Figure 6, bottom left). The calculated Brine Volume Fraction (BVF) was greatest in the bottom segment of ice and ranged from 2.6 to 24.6% of the total ice volume across the core (Figure 6, bottom right).

In Y2, level ice with visible discoloration from ice algae was selected near Point Barrow (71.37182°N, 156.55814°W). Snow depth in Y2 was less than in Y1 and ranged from 3 to 6 cm. Ice thickness showed minimal variability and ranged from 126 to 127 cm. PAR transmittance through the snow and ice was 1.8% of incoming radiation. Physical ice characteristics were similar to Y1 (Figure 6). Ice temperature decreased linearly from -16.9°C at the ice surface to -2.5°C at the ice bottom (Figure 6, top left). A "C" shaped profile was apparent in the bulk salinity profile (Figure 6, top right). Calculated brine salinity ranged from 40 to 183 and was generally highest near the surface and lowest near the bottom of the ice (Figure 6, bottom left). The calculated BVF was greatest in the bottom segment of ice and ranged from 2.6 to 20.9% across the ice core (Figure 6, bottom right).
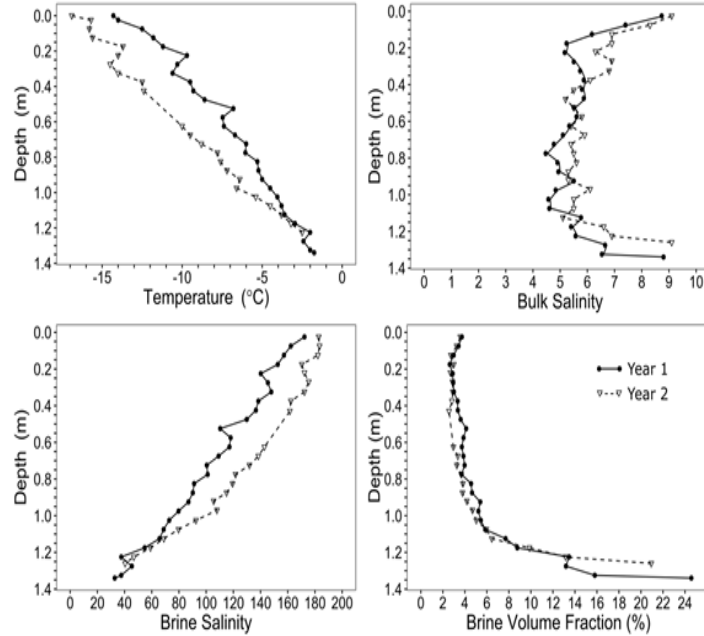
Figure 6. Physical properties of sea ice collected in Utqiaġvik, Alaska, in Y1 (2014) and Y2 (2015). Temperature and bulk salinity were measured while brine salinity and BVF were calculated according to Cox and Weeks (1983).

Biological variables

Biological data were collected for the bottom 10 cm of the ice cores taken from the landfast ice. In Y1, integrated ice Chl *a* concentrations ranged from 27.9 to 37.6 µg Chl *a* L^{-1} ice. Integrated EPS varied between 6,110 and 8,301 µg XGEQV L^{-1} ice, and bacterial abundances ranged from 2.3–3.6 x 10^8 bacterial cells L^{-1} ice. Within the bottom 10 cm, concentrations for all parameters were greatest in the lowermost 2 cm of landfast ice. In Y2, Chl *a* concentration in the bottom 10 cm of landfast ice exceeded the values from Y1 and ranged from 78 to 132 µg Chl *a* L^{-1} ice. EPS concentrations were 1.8 times lower in Y2 than in Y1. Sections again exhibited strong vertical gradients, with highest Chl *a* concentrations occurring in the bottom 2 cm of ice and highest EPS concentrations in the bottom 5 cm.

Tank Experiments

Abiotic variables

In Y1, ice thickness at OR-2 in was 16.5–21.4 cm from individual cores across all tanks and increased to 25.1–39.5 cm by OR+13. Surface irradiance was 20.1–103 µE m^{-2} s^{-1} and under-ice irradiance 9.1–14.6 µE m^{-2} s^{-1} throughout the experiment. In Y2, ice thickness in all tanks was 15.0–28.0 cm at OR-2 and 22.9–41.5 cm at OR+10. Surface irradiance was 230.2–307.2 µE m^{-2} s^{-1} and under-ice irradiance was 14.61–15.0 µE m^{-2} s^{-1} throughout the experiment. Brine salinity was greatest in the uppermost section of ice, ranging from 71–99 at OR-2 and 107–136 at OR+10 (Figures 7 and 8). Brine volume fraction was always greatest in the bottommost section of ice, ranging 4.7–24.1% at OR-2 and 2.4–20.8% at OR+10 (Figures 7 and 8).
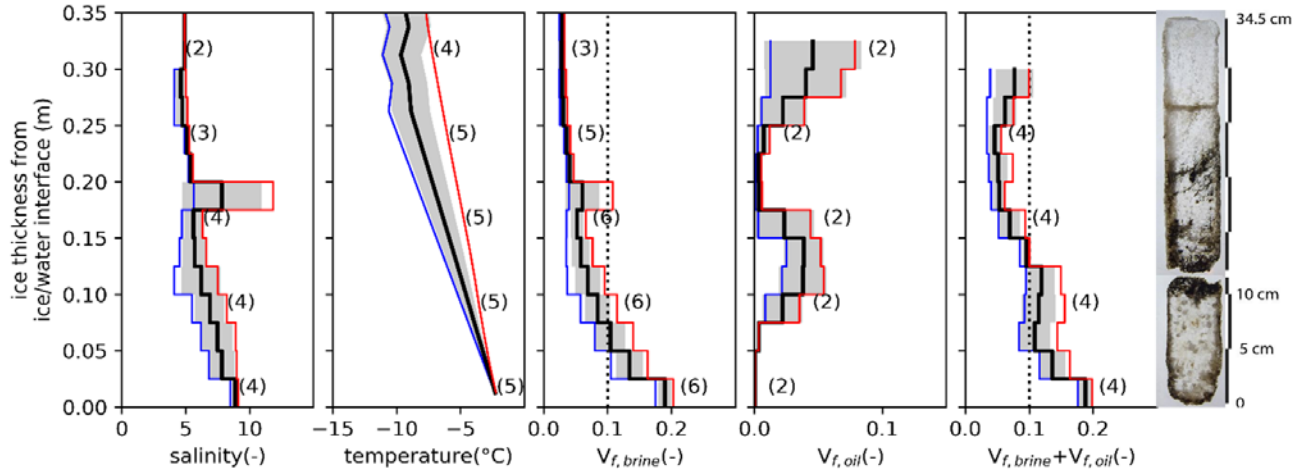
Figure 7. Sea ice physical properties for treatment BLY2 OR+10 and corresponding vertical section. For each property, minimum, mean, and maximum values are represented by blue, black and red lines, respectively, and the grey envelope represents 1 standard deviation. Numbers within parentheses indicate the number of samples collected at each depth. The vertical reference is set at the ice/water interface. Vf is the volume fraction.
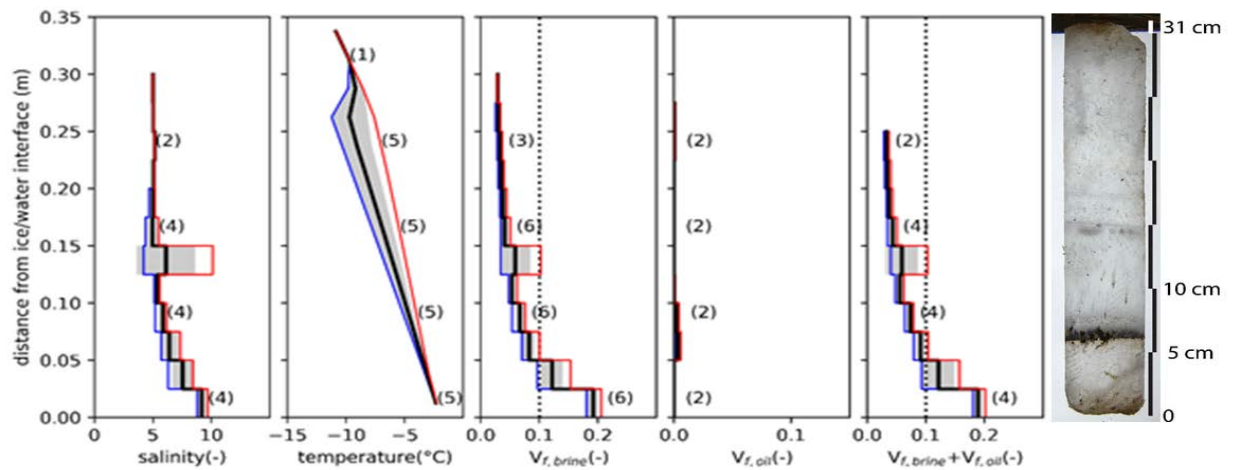
Figure 8. Sea ice physical properties for treatment EOY2 OR+10 and corresponding vertical section. For each property, minimum, mean, and maximum values are represented by blue, black and red lines, respectively, and the grey envelope represents 1 standard deviation. Numbers within parentheses indicate the number of samples collected at each depth. The vertical reference is set at the ice/water interface. Vf is the volume fraction.

During Y1, oil was observed reaching the ice surface within a day (Table 2). In most cases (BLY1a, b, and LY1a) oil moved through core holes drilled prior to oil release. However, surface oil spots >10 cm away from previous holes suggested oil had percolated through the ice matrix independent of migration along sampling artifacts (BLY1a, LY1b). Oil seeping between the ice and the plastic walls of the tank was observed in most treatments, including in Y2 (except oil emulsion treatments), but at a slower rate (<10 cm d^{-1}). Once the oil reached the surface through one of the artificial paths (walls or previous core holes), oil spread at the surface making observation difficult (BLY1, LY1, BLY2).

15

Migration rate was strongly reduced with smaller amounts of oil. For example, except for three spots visible at the surface BLY2a, oil did not surface through the ice matrix in the 5 mm thick oil lens treatment before oil started to pool after creeping up along the tank/ice interface (at OR+8). Oil failed to reach the surface of either EOY2 replicate through the ice matrix. In EYO2b, oil leaked through two unsealed core holes, one of which served as the point of oil injection.

Table 2. Timing and preferential movement path of oil surfacing through artificial ice.

Experiment		Surfacing time Δt (d)	rate v_{oil} (cm d^{-1})	Oil areal coverage %	Preferential oil *movement* path
LY1	a	0.6	28.8	95	Previous core hole, brine channel, walls
LY1	b	3.1	7.2	15	Walls, brine channels
BLY1	a	0.6	28.8	90	Walls, brine channels
BLY1	b	1.0	19.2	15	Previous core hole, brine channel, walls
BLY2	a	10.0	2.4	80	Walls, 1 brine channel
BLY2	b	10.0	2.4	80	Walls
EOY2	a	No surfacing[†]		<10[†]	-
EOY2	b	No surfacing		0	-

[†]: oil surfaced through the two core holes. Elapsed time Δt in days (d) between oil release and first surfacing of oil and average rate of oil movement V_{oil} (cm d^{-1}). Oil surface coverage at the end of the experiment is given in areal fraction (%). This number includes both oil migration through artifact structures, such as refrozen core holes drilled prior to the oil release and at the tank/ice interface, and through brine channels in the ice matrix.

We estimated the depth of oil penetration from cores and slabs in both the skeletal layer at the ice bottom and in the brine channel system (Figure 9). The number of cores and slabs, as well as the surface area, varied greatly from one treatment to another. Oil barely coated the skeletal layer in EOY2, and only one channel filled to 3 cm above the ice-water interface. The fine dispersion of oil droplets pervaded the skeletal layer. In BLY2, we observed one brine channel connecting the oil lens to the ice surface in a core. Additionally, a large number of smaller brine channels were filled with oil within 5 cm of the ice bottom, and some extended upward up to 20 cm from the ice/oil interface.

We calculated the density of channels occupied by oil as the number of oil-filled channels divided by the total surface area at any given penetration depth. With a larger amount of oil (BLY1, LY1), the density of brine channels containing oil that reached higher into the ice increased substantially (1.16 dm^{-2}) as did the average penetration depth. Ice within 5 cm of the ice/oil interface was fully saturated with oil; whereas, with smaller amounts (EOY2, BLY2), the oil remained within 2 cm of the oil/ice interface.
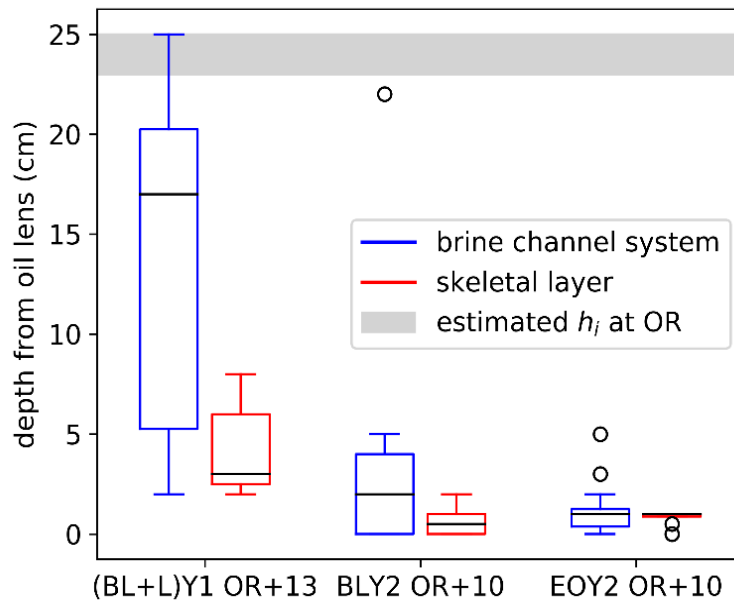
Figure 9: Oil penetration depth (cm) measured from the ice/oil interface for saturated brine channels (blue) and skeletal layer (red). Error bars are the smallest/largest depth within 1.5 interquartile range from the lower/upper quartile. Circles represent outliers.

Ice microstructure

From salinity profiles and coring observations, we expected a thin (2–3 cm) granular ice layer atop columnar sea ice. The upper 2 to 4 cm of ice was composed of small, randomly oriented ice crystals, with more air bubbles than occur in natural sea ice. Sea ice microstructure quickly transitioned to columnar sea ice. Biota inoculation perturbed the ice growth, with the introduction of the slush creating a thick layer (up to 3 cm). The microstructure consisted of small, randomly oriented ice crystals containing a large volume of air bubbles. Afterwards, ice quickly transitioned to columnar ice structure with preferentially oriented ice crystals growing (e.g., EOY2 at 7 cm). Just above the oil lens, the columnar structure was completely destroyed and a new layer of ice started growing, characterized by small, randomly oriented crystals (EOY2, 1 cm above oil lens). This corresponded to the baseline coring that introduced air and ice shavings below the ice, despite significant care taken to avoid disturbance.

The short period of time after each perturbation did not allow the ice to fully transition from granular to columnar sea ice. Hence, the average crystal size (1.2 +/-0.2 cm) estimated on the horizontal thin sections remained much smaller than in natural columnar sea ice.
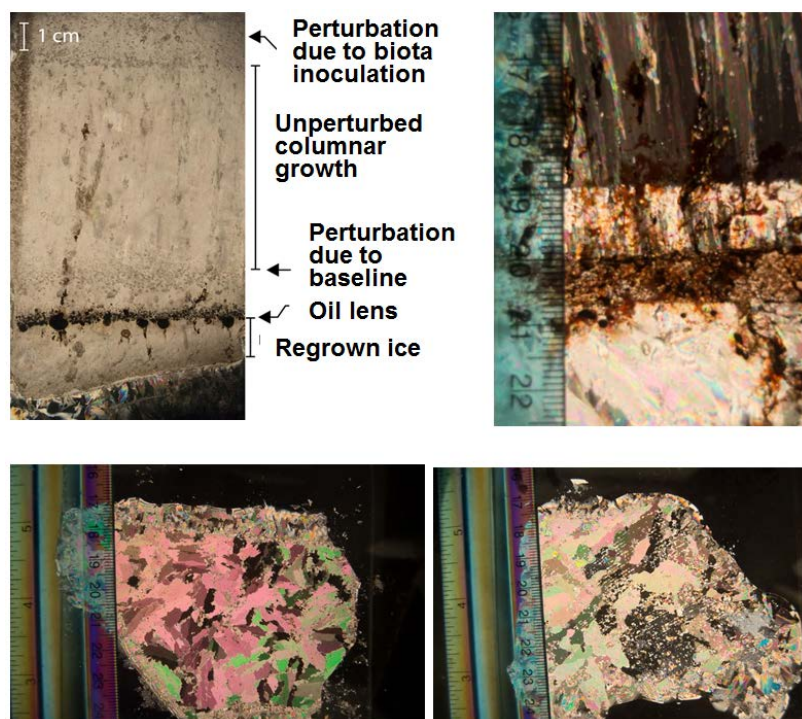
Figure 10. Microstructure of artificial and oil-contaminated sea ice; perturbed ice (above left), entrained oil/ice interface (above right), and horizontal cross sections (below).

Chlorophyll a

At OR-2, the BCY1 mean Chl *a* concentration was higher in the top ice section relative to the bottom section by a factor of 3. In BLY1, Chl *a* was also higher in the upper ice at OR-2 compared to the bottom ice section by a factor of 2. BCY1 and BLY1 bottom ice Chl *a* concentrations significantly decreased between OR-2 and OR+13 (LMER, $p<0.05$) while the surface sections did not significantly differ (LMER, $p>0.05$). The mean Chl *a* concentrations (LMER, $p>0.05$) for bottom ice sections did not differ significantly at OR+13 between treatments (LMER, $p>0.05$).

During Y2, maximum Chl *a* concentrations were nearly 25 times higher than in Y1. At OR-2, the highest concentrations were observed in the upper ice section, adjacent to the inoculation layer. This pattern changed over the course of the experiment and highest concentrations at the ice-water interface for all treatments were established at OR+10. Bottom ice Chl *a* concentration was significantly higher in the control (BCY2) compared to the oiled treatments (LMER, $p<0.05$; Figure 11).
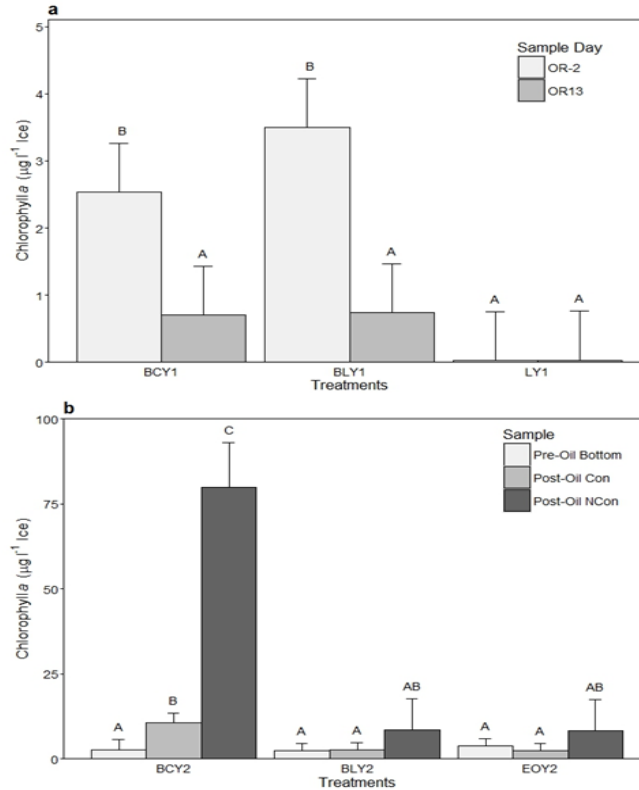
Figure 11. Mean chlorophyll a concentrations in (a) Y1 full ice cores and (b) Y2 bottom ice. Error bars represent the 95% confidence intervals. Letters above error bars represent Tukey's post hoc group assignment. Note different scales in Y1 and Y2.

Extracellular polymeric substances

In Y1, the EPS concentrations exhibited the same pattern as Chl *a* with higher mean concentrations in the topmost section of ice relative to the bottom section by factors of 1.5, 2.4 and 2.8 in the BCY1, BLY1 and LY1 treatments, respectively. EPS did not exhibit a significant difference across treatment or sampling day in the lowermost section of ice (LMER, $p>0.05$). In Y2, no vertical gradient in EPS concentrations was found at OR-2. Top ice sections were not significantly different among treatments or sample days (LMER, $p>0.05$), nor were bottom ice EPS concentrations (LMER, $p>0.05$). Ice formed after OR had significantly higher EPS concentrations in BCY2 than in EOY2 or BLY2 (LMER, $p<0.05$).

Algal abundance and species composition

The algal community composition in Y2 (not measured in Y1) was dominated by the pennate diatoms *Nitzschia sp.* and *Cylindrotheca closterium* at OR-2 across all tanks. At OR+10, the algal community composition remained similar to OR-2, dominated by *Nitzschia sp.* with low abundance of *C. closterium* (<1%). Algal cell abundance was significantly greater in the bottom and non-conserved bottom ice sections at OR+10 in the BCY2 treatment (LMER, $p<0.05$; Figure 12). Based on cell counts in the BCY2 treatment, a generation time of 0.2 doublings day^{-1} was calculated for the algae.
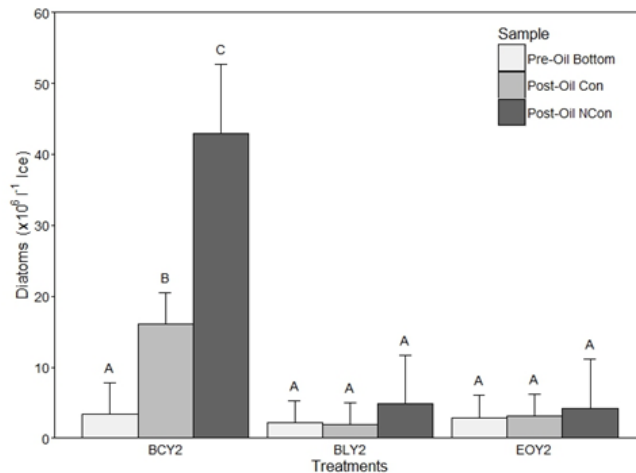
Figure 12. Mean total diatom abundance in bottom ice from Y2 experiment. Conservative (Con) indicates sections from the same depth relative to the air-ice interface; Non-Conservative (NCon) indicates sections from the same depth relative to the ice-water interface. Error bars represent the 95% confidence interval. Letters above error bars represent Tukey's post hoc group assignment.

At OR-2, empty frustules represented an average of 1.4% of all algal cells with high variability across tanks and cores. Empty frustule abundance at OR+10 increased across all treatments (Figure 13), and particularly in the oiled treatments, but was not statistically significantly different among treatments (LMER, $p>0.05$).

Cells deemed intact based on the epifluorescence observations (Figures 13 and 14) dominated algal cell abundance at OR-2 with 97–100% of all diatoms in full cores across treatments in Y2. In the BCY2 treatment, intact algal cells were most abundant in the ice section nearest the ice-water interface and lowest in the uppermost ice section at OR+10. In oiled treatments, intact algal cells were in lowest abundance in the ice formed post-OR, comprising 24–27% of total diatom abundance. Intact algal cells were significantly greater in the BCY2 treatment compared to the oil treatments at OR+10 (LMER, $p<0.05$).

Bacteria

Vertical differences in bacterial abundance in Y1 reflected those of Chl *a* and EPS, with highest abundances occurring in the uppermost ice sections, which were 1.8 and 3.5 times greater than bottom ice at OR-2 in BCY1 and BLY1, respectively. Abundance was opposite in LY1 with greater abundance in the bottom layer of ice. Bacterial abundance in bottom ice was significantly higher in BLY1 at OR+13 than LY1 and to all treatments at OR-2 (LMER, $p<0.05$). Bacterial abundance in BCY1 bottom ice was not significantly different from either BLY1 or LY1 (LMER, $p>0.05$).

In Y2, bacterial abundance was nearly identical between upper and lower ice sections prior to OR (OR-2) and lower than at the initiation of the experiment in Y1. Bacterial abundances did not significantly differ between treatments or sample periods when comparing top, bottom, and non-conservative bottom ice sections (LMER, $p>0.05$).
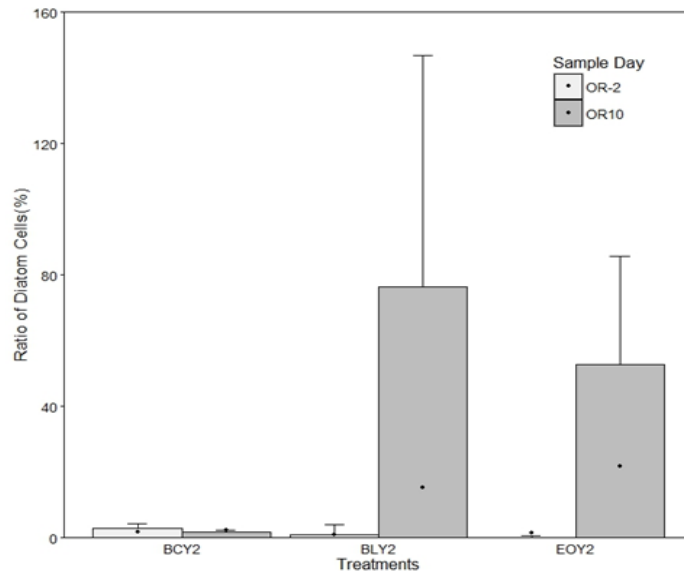
Figure 13. Full core mean percent "damaged" algae in Y2, as determined epifluorescently (bars). Point markers identify ratio of empty versus full diatom cells (%) (Frustules/Total Diatoms (excluding frustules)*100. Error bars represent the 95% confidence interval.
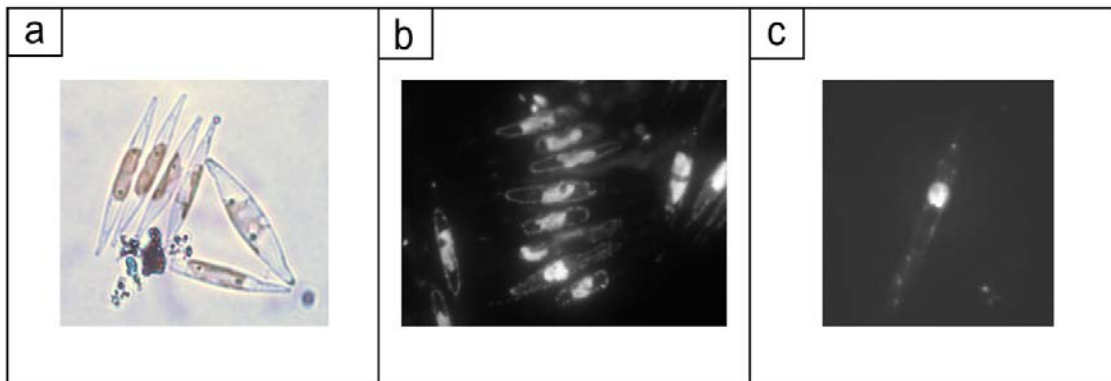
Figure 14. Diatom images: (a) Light transmittance image of *Nitzschia sp.* from unoiled tank at OR+10, (b) Epifluorescent image of "healthy" diatom cells from unoiled tank at OR+10 with elongated nucleus and intact plasma membrane, (c) Epifluorescent image of an "unhealthy" diatom cell from an oiled tank at OR+10 with tightly bundled nucleus and dissolved plasma membrane.

DISCUSSION

Overview

During the course of this project, we made substantial advances in designing and implementing mesocosms for the controlled growth and contamination of artificial sea ice. Mesocosms designed for this experiment were successfully employed to grow sea ice with physical properties and biomass representative of early to mid-spring fast ice found along the Alaskan Arctic coast. Using these tanks, we increased the understanding of processes related to the migration of oil through the porous structure of sea ice and the impacts on the biota within the ice. In particular, we found that North Slope crude oil penetrated much further into the overlying ice than observed in other studies (NORCOR, 1975, Glaeser and Vance, 1972), and the oil migration rate we observed was proportional to the thickness of the oil lens. This suggests that ice in the immediate vicinity of a large spill could quickly become infiltrated with oil, even at very low temperatures. Finally, we observed considerable negative impacts of oil to natural sea ice biota exposed to oil, especially diatoms, which are a critical component of the Arctic food web. We identified a new microscopic technique to estimate the physiological impact of oil exposure on diatoms and found that up to 75% of oil-exposed cells exhibited signs of cellular damage. Other methods showed that diatoms exposed to oil were completely inhibited in their growth compared to unoiled controls. These findings suggest an oil spill is likely to have lingering and long-lasting negative effects on the fate of the sea ice biological community.

Similarity between Natural and Artificially Grown Ice

Abiotic factors

For our results to be reliable, we needed to be sure that the artificial ice we were growing accurately reflected natural ice in both its geophysical and biological properties. The thermal and salinity profiles of sea water define the environment that sea ice organisms reside in. Important factors include available surface area, which impacts attachment (Krembs et al. 2000); brine channel diameter, which constricts movement (Weissenberger et al. 1992); and local salinity, which affects osmotic regulation and growth (Cox and Weeks 1983; Zhang et al. 1999). Brine Volume Fraction (BVF) plays an important role in oil infiltration in sea ice, which made it important to have realistic BVF profiles for this oil in ice experiment.

Temperature and bulk salinity work together to control the brine salinity and brine volume fraction (Cox and Weeks 1983; Leppäranta and Manninen 1988), so it was important that temperature and salinity profiles in our artificial ice reflected field conditions. As observed in early spring conditions in other fast ice studies (e.g., Cota et al. 1991; Gradinger et al. 2009), ice temperature profiles from the Utqiaġvik fast ice sampled for this study were relatively linear (Figure 6). The temperature profiles of the artificial sea ice were also linear. Bulk salinity profiles determined for Utqiaġvik fast ice followed the characteristic C-shaped profiles of first-year ice prior to the onset of melt, with elevated salinities at both the ice-air and ice-water

interfaces (Figure 6; Malmgren 1927). While we also observed the typical C-shaped bulk salinity profiles in our experiments, they were modified by the additions of oil (Y1 and Y2) and biota (Y2).

Brine salinities within the tanks fell within the range of natural fast ice, with highest salinities near the cold surface and low values in the lowermost sections ranging from 41–160. Maximum ice algal photosynthesis occurs at salinities between 35 and 51 (Ralph et al. 2007), while salinity in excess of 90 can inhibit algal growth (Zhang et al. 1999). Sea ice algae in the upper sections of the ice in both field and tank environments likely experienced salinity stress as a result of high brine salinities. Ice samples collected throughout the experiments contained segments above the salinity inhibition threshold of 90 (Figures 7 and 8).

BVF profiles under thermodynamic growth exhibited an L-shape (Figures 7 and 8). Field and tank brine salinity profiles were similar to one another in shape and magnitude of values, disregarding a spike in BVF at the ice-air interface in Y1 at OR-2. This spike was likely due to upward brine expulsion during freeze up resulting in a hypersaline fluid on the surface of the ice (Perovich and Richter-Menge 1994).

Biotic factors

We selected our biological collection site in a location with a moderate snow depth to increase our chance of encountering high algal biomass (Mundy et al. 2005). Under-ice PAR measured in Y1 and Y2 was typical of Arctic first-year ice in late April (Gosselin and Legendre 1990; Manes and Gradinger 2009; Gradinger et al. 2009). Chl a concentrations measured in our tanks fell within the range of values reported for other sea ice tank experiments (Table 3) and natural environments. The highest recorded Chl a (106 µg L^{-1} ice) for a tank experiment was documented after 35 days in 180 L outdoor tanks (Weissenberger 1998). Although our experiments were run for considerably shorter time periods, the observed algal growth suggests that higher biomass could have been achieved with longer incubations. The Chl a values in Y2 test tanks prior to oil inoculation were similar to the first-year ice at the beginning of spring, February–March, in coastal Alaska waters (Lee et al. 2008; Manes and Gradinger 2009). Other experiments (Krembs et al. 2001; Mock et al. 2002) were conducted with similar initial Chl a concentrations to our own but differed in incubation period. The final Chl a concentrations in our tanks were similar to the beginning ice algal spring bloom conditions in the field and exceeded most summer pack ice values (Gradinger 1999; Lee et al. 2008; Manes and Gradinger 2009; Gradinger et al. 2009).

Algal cell concentrations in our tank experiments were generally within the range of values reported for other tank studies and environmental samples (Tables 3 and 4), reaching maximum abundances of over 30 x10^6 cells L ice^{-1}. Further growth of algae, as the result of sufficient light and inorganic nutrient conditions, led to increased abundances over time in the tanks, with final values exceeding field data from central Arctic pack ice by a factor of 2 (Gradinger 1999),

though lower than our field sample concentrations in spring. By growing algae within the sea ice to environmentally relevant concentrations, meaningful data relating to oil spills were collected.

Algal diversity in Arctic sea ice varies greatly between locations and with time but is typically dominated by pennate diatoms (Poulin et al. 2011). The importance of biodiversity in contributing to ecosystem resilience after a trauma (e.g., oil spill) has been well documented (Folke et al. 2004). Despite incubation with natural ice biota, tank algal diversity was low and the community was almost exclusively dominated by the single pennate diatom *Nitzschia sp.* (99%), followed by *Cylindrotheca closterium* (1%). The pennate diatom genus *Nitzschia* is commonly associated with sea ice in Arctic and Antarctic marine systems (Suzuki et al. 1997; Ratkova and Wassmann 2005). A possible explanation for the low algal diversity observed in our study is that supplementation of biota with laboratory-grown cultures led to an overwhelming inoculation of culture/tank adapted algae that were capable of out-competing other algae for resources. However, it should be noted that *in situ* species richness in individual ice floes was also considerably below the 1,027 species of algae reported in Arctic sea ice by Poulin et al. 2011. Hsiao (1980) reported 196 species of ice algae during his study of Canadian landfast ice, and 55 taxa were identified by Horner and Schrader (1982) in Beaufort Sea landfast ice. Thus, field studies demonstrate the local selection of a limited number of species matching the current environmental conditions observed in our study.

Like Chl *a*, extracellular polymeric substances (EPS) concentration in the ice tanks increased with time and reached values similar to early spring landfast ice levels. EPS in sea ice are largely produced by sea ice algae and bacteria and may have a cryoprotective role (Krembs et al. 2002; Nichols et al. 2005; Aslam et al. 2012b). The initial EPS concentrations in the tanks were below most reported field data for bottom ice by one order of magnitude. Riedel et al. (2006) report similar concentrations prior to the spring ice algal bloom (i.e., to mid-March under low snow cover or mid-May under high snow cover). The moderate correlation (R^2=0.43) between diatom abundance and EPS concentrations in unoiled samples indicates that diatoms were likely the source for the bulk of EPS production in our study, as suggested by Krembs and Engel (2001) and Riedel et al. (2006).

Bacterial abundances established in the experimental tanks fell within ranges reported for other field and experimental studies (Tables 3 and 4). In Arctic fast ice, bacterial abundances span several orders of magnitude from early spring into summer (10^7 to 10^9 cells L^{-1} ice) with no temporal trends (Krembs et al. 2002; Riedel et al. 2006). Other experimental studies reported either similar bacterial abundances (Aslam et al. 2012b) or substantially higher abundance (Weissenberger 1998). The high abundances of bacteria in the non-seeded LY1 treatment could have resulted from contamination from other tanks, non-sterilized water supplies and/or the artificial seawater salts used, a problem that cannot be excluded in open tanks in standard cold rooms and environmental chambers.

Table 3. Sea ice tank studies that cultivated biota comparable to this study. Bold values indicate the maximum value during the experiment.

Study	Reservoir Type	Tank Volume (m^3)	Section (cms)	Ice thickness (cm)	Incubation (days)	Chl a (μg L ice^{-1})	Algal Abundance (cells L ice^{-1})	Bacterial Abundance (cells L ice^{-1})	Chl a (mg m^{-2})	Algal abundance (cells m^{-2})	Physical data on ice
Weissenberger 1998	Tank	0.18	Full Core	15	35	106	37×10^6	0.6×10^{12}	20	8×10^9	minimal
Weissenberger 1998	Tank	0.18	Full Core	29	42	49	24×10^6	0.6×10^{12}	15	35×10^9	No
Weissenberger 1998	Tank	0.18	Full Core	22	91	80	14×10^6	0.7×10^{12}	21	4×10^9	No
Krembs et al. 2001	Basin	180	All Sections	21	17	0.1-2	0.79×10^6	na	na	na	Yes
Mock et al. 2002	Tank	4	All Sections	15	10	3-4	na	na	na	na	Yes
Aslam et al. 2012	Basin/ Dividers	216/1.2	All Sections	10	5	na	na	0.8×10^9	na	na	Yes

Table 4. Sea ice field studies that measured biota comparable to this study. Dash represents no data collected for the study.

Study	Ice Type	Location	Year	Ice Thickness (m)	Chl a (µg L^{-1} ice^{-1})	Algal Abundance (cells L^{-1} ice^{-1})	Bacterial Abundance (cells L^{-1} ice^{-1})	EPS (mg XGEQV L^{-1} ice^{-1})	Chl a (mg m^{-2})	Algal abundance (cells m^{-2})	Bacterial Abundance (cells m^{-2})
Gradinger et al. 1999	Pack Ice	Greenland Sea	1994	--	--		--	--	0.1-3.3	1547 x 10^6	20.5 x10^{11}
Gradinger 1999	Pack Ice	Greenland Sea	1991, 1994	01-6.7	0-109 mean	0.4 -18.0 x10^6 mean	--	--	0.01-7.09	320-14,100 x10^6	--
Gradinger et al. 2005	Pack Ice	Beaufort Sea	2002, 2003	0.9-2.7	0-11	--	--	--	0.1-1.7	--	--
Lange et al. 2015	First-year ice	Lincoln Sea	2010-2012	0.83-1.77	0.01-15.4 mean 0.6	--	--	--	mean 0.7	--	--
Lange et al. 2015	Multi-year ice	Lincoln Sea	2010-2012	2.23-3.11	<0.01-14.1 mean 0.2	--	--	--	mean 0.4	--	--
Krembs et al. 2002	Fast Ice	Utqiaġvik, AK	1999	0.4-1.65	<0.1-16 (March only)	--	2.5-7 x10^7 (March only)	1-7.7	--	--	--
Riedel et al. 2006	Fast Ice	Beaufort Sea	2005	1.3-2.0	0.3-711 median 88.4	--	0.3-4.3 x10^9 median 1.7 x10^9	<0.1-10.5 median 1.36	--	--	--
Lee et al. 2008	Fast Ice	Utqiaġvik, AK	2002, 2003	--	--	--	--	--	1-895	--	--
Gradinger et al. 2009	Fast Ice	Utqiaġvik, AK	2002, 2003	--	15-340	--	--	--	--	--	--
Krembs et al. 2011	Fast Ice	Utqiaġvik, AK	2001, 2002	1.57-1.62	12.3-55.1	--	--	2.0-5.5	--	--	--
Manes & Gradinger 2009	Fast Ice	Utqiaġvik, AK	2005, 2006	0.47-1.59	0.3-696	--	--	--	--	--	--
Hsiao 1980	Fast Ice	Canada	1971-1978	--	--	--	--	--	--	--	--

Geophysical Effects of Oil in Sea Ice

The extent of oil penetration during the growth season in this study was larger than reported in other studies. According to a previous experiment (Karlsson et al. 2011; Pringle et al. 2009), with the ice porosity remaining below 10%, neither brine nor oil should have been mobile or capable of migrating vertically through the full extent of the ice. However, within two days of the oil release, oil surfaced through independent brine channels at several locations of the ice surface. Under natural conditions, such oil movement has only been recorded in warm ice, with only a few oil droplets and limited oil percolation within the brine channels up to 20 cm above the oil/ice interface in cold ice (T_{ice} < -5°C) (Martin 1979; Dickins et al. 2006). No occurrence of migration through cold ice has been reported for laboratory grown sea ice (Karlsson 2009; Martina et al. 2016).

One reason we may have observed deeper oil penetration in ice compared to other studies is due to differences in ice structure between our ice and naturally formed ice. In most respects, our artificial ice was similar to natural ice, with linear temperature profiles during the growth season. However, despite a salinity profile exhibiting the typical C-shape curve with higher salinity at both interfaces (Eicken 2003), the granular ice layer was at least three times thinner (<4 cm) than ice grown under natural conditions, which usually ranges from 10 to 15 cm (Galley et al. 2015; Weeks 2010; Zubov 1943). In the absence of turbulence at the water surface, the transition from granular to columnar ice occurred within a couple of centimeters in the artificial ice and most of the ice was columnar. Our experimental protocols were in line with other studies where columnar sea ice was artificially grown by seeding the ice surface (Dickins et al. 2005; Pringle et al. 2006; Karlsson 2009).

Most of the thickness of Arctic sea ice is made of columnar ice topped with a thin layer of granular ice. Within the columnar ice, brine channels extend upward from the ice bottom in a density estimated to be about 100 m^{-2} (Lake and Lewis 1970) and with a diameter of a few millimeters. The brine channels that extend up to the transition between granular and columnar sea ice form many potential migration pathways for brine (Cole and Shapiro 1998) and oil. In granular sea ice, pore size distribution is skewed towards smaller pores relative to columnar ice (Eicken et al. 2000), and the presence of sub-millimeter and smaller is more likely to hinder movement of brine and oil. Thus, the likelihood that some path exists in the granular layer in which oil can freely move increases as the granular layer thickness decreases.

Oil viscosity is a critical property that can determine oil redistribution within the brine channel system (Karlsson 2009). The oil used in this experiment remained fluid at -73°C, at odds with the lab report provided by SL Ross Environmental Research Ltd. It exceeded the pour point of 59 diverse oils whose properties were compiled by the International Tanker Owners Pollution Federation Limited (ITOPF 2011). This temperature dependent property suggests that the Alaska North Slope (ANS) crude oil used in this experiment could have penetrated farther into the brine

channel system than other oils would be capable of at similar temperatures, potentially influencing biological processes.

Biological Effects of Oil in Sea Ice

We tested two types of oiling scenarios to simulate different methods of release into the environment. One case would be oil released from a capsized vessel, which would behave differently than a vigorous wellhead blowout. Both scenarios are capable of contaminating sea ice at the ice-water interface. A full-scale blowout, as witnessed during the Deepwater Horizon and Ixtoc 1 spills in the Gulf of Mexico, can emulsify the oil and produce droplets <300 µm in diameter (Masutani and Adams 2000). By contrast, a sunken vessel or a slow leaking pipeline would produce much larger droplets that can coalesce at the ice-water interface to form an oil lens (AMAP 2010). Even slow leaks can be mechanically dispersed by wave energy at the ocean surface to produce small droplets that will settle out over a prolonged period of time (Farmer and Li 1994; Zheng and Yapa 2000). Oil released under sea ice in our experiments had strong negative effects on ice algal growth, while the abundance of bacteria remained similar across treatments regardless of the route of oil exposure.

Effects on sea ice algae

We observed a substantial inhibition of algal growth and decreased diatom abundance in the bottom of oiled ice compared to control ice (Figure 11 and 12). These results could be explained by a combination of inhibition of cell growth and division (Hsiao 1978; Aksmann and Tukaj 2008; Gilde and Pinckney 2012) and reductions in Chl *a* concentration per cell (Cullen et al. 1993). We also observed increases in damaged diatom cells in oiled ice compared to control ice (Figures 13). These results indicate that both lens and emulsified oil treatments harmed the biological community within the ice and halted the algal bloom that was induced in the artificial sea ice tanks. The effect persisted in the emulsified treatments, suggesting that an oil spill under sea ice during spring or summer could cause long-lasting negative impacts on the biological community in the ice, even quite far from the initial spill, as wind and wave action spread the oil thinly across the bottom of the ice. Further work is needed to determine the minimum oil concentrations necessary to inhibit the growth of the ice algae.

Currently, three oil inhibition pathways have been suggested for algae in general: direct adsorption to individual cells reducing nutrient and gas exchange (Jiang et al. 2010), toxicological interactions with cell membranes and photosystem components (Singh and Gaur 1988; Aksmann and Tukaj 2008; Perez et al. 2010), and reduction of light transmittance. We propose a fourth interaction unique to sea ice: plugging of brine channels by oil from below the ice, thereby isolating algae from seawater exchange and reducing or eliminating replenishment of inorganic nutrients, oxygen, and CO_2 from the underlying water mass. All four mechanisms would be most pronounced in the basal 1–2 cm where most of the biological interactions occur in natural ice habitats. The toxicological impact could extend further into the ice due to fluid convection, dependent on brine channel connectivity.

Extracellular polymeric substances are typically contributed by algae and bacteria in sea ice (Riedel et al. 2006; Collins et al. 2010; Krembs et al. 2011). We demonstrate for the first time that EPS production was inhibited by crude oil exposure. EPS protects diatoms and bacteria from freezing and from hypersaline environments like high salinity brines (Aslam et al. 2012a; Liu et al. 2013), and it could function similarly under hyposaline exposure such as meltwater flushing (Ozturk and Aslim 2010). EPS is also produced by algae as a stress response to temperature, nutrient limitation (Alcoverro et al. 2000), and oxidative stress (Chen 2014). EPS can directly influence salt retention in sea ice by increasing the abundance and size of brine pores (Krembs et al. 2011). Such effects can alter the distribution of oil and its water-soluble fraction within the ice, thus impacting oil exposure to the microorganism inhabitants of the ice. Theoretically, EPS production could protect cells from crude oil exposure, as has been found for bacteria exposed to heavy metals (Bitton and Freihofer 1978), by surrounding the cells and providing a diffusive barrier against crude oil compounds. A cessation of EPS production makes this protective mechanism unlikely to protect cells at high oil doses in the ice matrix. Reduced EPS concentrations also affect sea ice microstructure and permeability (Krembs et al. 2011), potentially increasing the flow of oil into the brine channel network.

Our study clearly demonstrated biological effects of oil exposure in sea ice systems. Based on our observations, we propose two possible methods for determining cell damage and mortality that could be applied to fixed melted sea ice samples in field studies: the frequency of empty diatom frustules and fluorescent cell properties. We assume that empty silicate frustules are retained within the ice matrix after diatom cell death. The frustule abundance, therefore, represents at least a fraction of the total dead cells as a consequence of oiling. This relationship between relative frequency of dead algal cells and oil exposure has been observed in other studies (e.g., Echeveste et al. 2010; Gilde and Pinckney 2012). Empty frustules as an indicator of cell death certainly underestimates actual mortality. Nevertheless, we observed a clear signal in the relative empty frustule abundance as it increased after oil exposure.

Frustule abundance may be a particularly suitable metric for sea ice communities, which are often dominated by diatoms as main primary producers. Echeveste et al. (2010) found that by using membrane permeability digestion assays, most marine algae showed increased mortality when exposed to two common PAHs and that natural communities showed substantially more cell death than lab cultures. Because most, if not all, of the algal growth in the artificial sea ice was derived from lab cultures, these impacts may be even greater in a natural setting.

A second measure became evident during the fluorescence studies of fixed samples. Two groups of cells could be clearly separated: Group 1 (intact) demonstrated strong plasma membrane fluorescence with an indiscernible nucleus shrouded by the chloroplasts, and Group 2 (damaged) lacked a fluorescent plasma membrane, had weak or no chloroplast fluorescence, and had a more defined nucleus (Figure 14). The fluorescent dye DAPI is specific to DNA and partially to RNA and is known to stain chloroplasts (Selldén and Leech 1981), mitochondria (Williamson and Fennell 1979), and nuclear DNA (Porter and Feig 1980). So far, viability assays of

phytoplankton rely on specific stains (Roth et al. 1997; Veldhuis et al. 2001) or digestive enzymes (Agusti and Sánchez 2002) that penetrate compromised cell membranes for easy viewing in unfixed samples. For example, Echeveste et al. (2010) utilized a membrane permeability test which digests the permeable membranes of dead cells. In this method, two sets of pseudo-samples are enumerated: one counting of both live and dead cells, and one counting only the living cells. These processes will not work with fixed field samples because the plasma membranes become permeabilized in 20 to 120 minutes after being fixed in formaldehyde (Veldhuis et al. 2001). We could not confirm whether the observation in our experiments represented dead or damaged cells nor determine a mechanistic action. However, the oiled tanks had higher proportions of intact cells than damaged cells. Veldhuis et al. (2001) determined that non-viable cells still possess their photopigments and that loss of membrane integrity occurs later as a process of unicellular automortality, synonymous to apoptosis in multicellular organisms. We suggest that the capacity to visualize cell damage at the time of formaldehyde fixation is possible using only DAPI cell staining. We propose that the possible new methods be further developed and rigorously validated to determine the efficacy of this method to determine cell damage caused by oil. A post-fixation method for determining cell damage after an oil spill will enable investigators to ship samples from a location of incidence to an analytical lab, freeing valuable time during a critical and time-sensitive period.

Effects on bacteria

The temporal changes of bacterial abundance in oiled and controlled treatments varied markedly between experiments and ice sections. In Y1, when no algal growth occurred within the ice and nutrients were not supplemented, bacterial abundance increased by a factor of seven in the bottom ice of the BLY1 treatment over time. This increase can possibly be explained by growth stimulation of oil-degrading microbes. Bacterial abundance was previously observed to increase after light dosing with diesel and crude oil in natural Antarctic landfast sea ice (Delille et al. 1997), Antarctic planktonic environments (Delille et al. 1998), and soils in the Antarctic (Delille 2000).

Interestingly, in contrast to Y1, bacterial abundances in Y2 were not enhanced by oil introduction, and we observed substantial ice algal growth in the unoiled treatment BCY2. One reason could be that oil incubation was three days longer in Y1 than in Y2. This period, though short, could have allowed for an additional 3.6–5 divisions of bacteria (based on bacterial growth rates at 0°C; Kuparinen et al. 2011) and could explain differences between Y1 and Y2. Alternatively, since bacteria and algae compete for inorganic nitrogen sources, enhanced algal growth in Y2 might have caused nutrient depletion for bacteria. Additional factors such as grazing mortality or viral lysis (Thingstad and Lignell 1997) were not assessed in this study but could have contributed to stimulating the microbial food web within the ice (Vézina et al. 1997). No difference was found in bacterial abundance between the two oil treatments (dispersed and non-dispersed), which was unexpected as breaking oil into small droplets is the main principle behind the use of chemical dispersants to promote biodegradation of spilled oil (Prince et al.

2013). By dispersing oil, more surface area is exposed for bacterial attachment. Bacteria have been shown to grow faster and to a greater abundance with the use of chemical dispersants at cooler temperatures (10°C) relative to oiled controls. We suggest that nutrient competition or heterotrophic top-down control superseded the difference between the two oiled treatments.

Lessons Learned: Ice Tank Design

Although we based our tank design on previous examples, there were many engineering details that had to be learned along the way to obtain high-quality artificial sea ice. Here we offer some of the lessons learned about the design and operation of these tanks.

Wall effects represent an unnatural aspect of all tank experiments, and their impact is dictated by the size, shape and internal color of the tank (Martín-Robichaud and Peterson 1998). Tank wall color was a major variable influencing the light field relevant to biological processes. White tank walls allow for higher light intensities, whereas black tank walls allow for more natural light gradients through the ice layer but require stronger LED intensities. Black tank walls might be specifically recommended for conducting experiments with phototactic biota, while white walls could be beneficial to studies where simulating a natural light field is deemed less important than achieving an adequate light quantity.

Our pressure-release mechanism (Figure 3) using antifreeze functioned well in most tanks except for a single catastrophic failure in Y2. A siphon was formed, presumably due to the release of a small ice blockage in the tube, releasing the majority of the antifreeze. This resulted in the desalination of the ice within one of our tanks. Upon discovery, a small hole was drilled at the highest point of each pressure release to ensure that no siphon could form in the future.

The oil used in this experiment displayed physical characteristics at odds with its stated properties, in that the oil was very fluid even at very low temperatures. A small aliquot was frozen at -80°C and retained fluidity. While not a rigorous pour point test, this led us to believe that the oil used in these experiments might not represent the bulk properties of the crude oil from which it was derived. It may be that unmixed oil may begin to separate, allowing a lighter, more fluid portion to accumulate at the surface where we collected our oil.

Lessons Learned: Biological Inoculation and Growth

The rate of ice growth is largely driven by the temperature difference between water and air and the thickness of the ice cover. Growth rates of Arctic first-year ice predominantly range from 0.5–2 cm d^{-1} (Nakawo and Sinha 1981). In Y1, the ice growth rate in the tank at the time of biological inoculation was 5 cm day^{-1} and was slowed in Y2 to 1 cm day^{-1}. Biological processes can also be affected by the rate of ice growth. If ice grows too fast, ice biota can become encapsulated within the ice sheet where they might be exposed to low temperatures and high brine salinities (Cox and Weeks 1983; this study in Y1). The measured gliding rate of the sea ice diatom *Cylindrotheca closterium* was on average 14.4 cm day^{-1} at a temperature of 0°C (Aumack et al. 2014). Freshwater diatoms have even higher gliding rates, ranging from 35–109 cm day^{-1} at

their optimum temperature and much slower speeds at cooler temperatures (Cohn et al. 2003). Our ice growth rates were within the range of these gliding rates, yet we found a layer of dead cells in the inoculation layer of Y1. This may have been attributed to unaligned crystals representative of granular ice creating a tight network of interlocking crystals with minimal connectivity of brine pockets (Bock and Eicken 2005). It is not until congelation ice forms that vertically aligned crystals and brine channels would have allowed for easier navigation by ice algae.

By controlling the maximum thickness of ice in our tanks, we ensured that algae remained capable of continued growth in the water and in the bottom ice layer. In experiments, ice growth can be controlled by modifying the air or water temperature or a combination of the two. The restricted range of cold room temperature settings of our experimental chamber limited our ability to slow initial ice growth. The use of submersible in-tank heaters was applied to control ice growth rate. Lateral cooling along the tank walls was successfully limited by insulating around the tanks (Figure 3). Water heating systems in both years were somewhat unsatisfactory. The use of multiple heaters in each tank in Y2 allowed for variable heating but likely caused the larger variability of ice thicknesses across tanks. Inter-tank ice thickness variability was unsatisfactory. We believe that the heating elements varied in their actual heat output and not representative of the manufacturer's specifications. In the future, it is recommended that high quality, precision heaters be used within the tanks to limit the difference in ice thickness between tanks. Our target ice thickness of 35 cm in the tank experiments was a compromise between forming ice sufficiently thick for algal growth while limiting the increase in water salinity below the ice (due to ice desalination), which could decrease algal growth rates. Sea ice algae exhibit maximum growth rates at salinities between 30 and 50, while most taxa become inhibited around 90 (Zhang et al. 1999)

Successful inoculation of ice tanks with sea ice biota is a prerequisite for conducting the type of experiment presented here and was, in hindsight, the most considerable challenge in this experiment. Our initial goal was to mimic the processes in nature, where Arctic sea ice is populated with a diverse assemblage of bacteria, algae, and metazoans through initial seeding followed by succession. These organisms are incorporated into the ice during freeze up (Reimnitz et al. 1993; Gradinger and Ikävalko 1998) or recruit to the ice after it has formed (McConnell et al. 2012). Subsequently, the sea ice community changes over time as flora and fauna are exposed to temperatures less than the freezing point (-1.8°C at a salinity of 35) and salinities 2–7 times greater than seawater. Previous experiments have taken different approaches in regards to organism collection and incubation. The most relevant inoculum source for sea ice studies is arguably from the sea ice itself. Krembs et al. (2001) utilized both melted ice cores and brine collected from sea ice and incubated the samples for three months to aid in biomass development. Weissenberger (1998) utilized sea ice brine along with natural seawater to inoculate tanks, while Mock et al. (2002) relied solely on large cultures of sea ice derived algae grown in the lab. An alternative to sea ice derived biota is to utilize natural seawater (Zhou et al. 2014).

The method of inoculation was common to all of these experiments and involved biota being suspended in the tank water prior to freezing. Since our experiment also attempted to establish a diverse and natural sea ice community, we added communities from landfast sea ice, supplemented in Y2 with laboratory-grown ice algal cultures. The initial pouring of the inoculum over a slush ice layer was ineffective as biota froze into the ice and remained trapped in the surface ice, resulting in low biota concentrations near the ice-water interface. Such freeze-in events have been observed in natural and experimental sea ice during freeze up when frazil ice rises through the water column entraining biota (Gradinger and Ikävalko 1998; Weissenberger and Grossmann 1998). A frazil layer was added below already formed sea ice of a thickness of 10 cm to provide the biota an environment of slow ice growth and reduced the risk of rapid freezing. The coarse ice crystals used in our experiment fell into the size-range of natural frazil ice crystals, which span several orders of magnitude from 1×10^{-2} to 1×10^{2} mm with a common range of 2–3 mm (Smedsrud Henrik 2001). A secondary inoculation was conducted 24 hours later with a slow release of the biota just below the ice in a density-stratified layer, which acted to hold the biota in contact with the ice. The combination of these two methods was successful and ice algae grew in the ice bottom layer with little initial variability among tanks. However, a limitation of this method is the interruption of columnar ice growth and potential disruption of brine channel connectivity.

We conducted oil toxicity experiments on meiofauna using a water accommodated fraction assay, but high initial mortality in the controls led to uninterpretable results. We suspect that specimens utilized during the toxicity experiments sustained damage during handling and transport from the field. Organisms used for these experiments were first transported in bulk and incubated in the cold room for several days before toxicity testing experiments began. The fragility of these organisms suggests that toxicity experiments should be conducted as soon as possible after collection, ideally without air transport. Future experiments of this nature would likely be more successful if conducted at the Barrow Arctic Research Center in Utqiaġvik. Future experiments should also time the collection of samples to periods with high initial concentrations of meiofauna. Since these organisms are patchy in time and space, very large collections of ice are needed to obtain a suitably large initial population for toxicity studies.

CONCLUSIONS

This study demonstrated that sea ice mesocosms can be used for controlled experimental studies of sea ice geophysics and oil impacts on ice biota. Novel approaches for inoculation of growing artificial ice sheets with field sampled biota were developed and biological characteristics matching natural conditions, specifically ice algal biomass, were achieved and maintained. Two different potential oil spill scenarios (oil lens under ice and dispersed oil droplets) were successfully simulated inside the tanks. A comparison between tanks with and without oil exposure allowed studying biological effects on sea ice algae, bacteria, and the production of EPS.

In the case of an environmental oil spill, the Natural Resource Damage Assessment of NOAA (https://darrp.noaa.gov/about-darrp/natural-resource-damage-assessment) requires identification of the damage, as well as an assessment and plan for restoration and monitoring. In terms of damage, this study suggests that oil spills during the ice algal bloom season can disrupt ice algal growth, which could lead to negative effects within the Arctic ecosystem on higher trophic levels, since ice algae provide an abundant and early food source for pelagic zooplankton (Michel et al. 2006; Søreide et al. 2010; Durbin and Casas 2014) and benthic fauna (Boetius et al. 2013). Furthermore, ice algae may seed the annual phytoplankton bloom (Haecky et al. 1998; Jin et al. 2007; Szymanski and Gradinger 2016), which could be delayed or reduced under an oil spill scenario. Coupling measurements of both the pelagic and benthic ecosystem after an oil spill in icy conditions will be crucial for determining impacts to these realms. Advection of phytoplankton into the area of an oil spill may act to mitigate the loss of a localized phytoplankton seed population. If an oil spill were to occur during peak bloom, the ice algae could become contaminated by the crude oil source and enter the food web either through adsorption or as an accumulation of toxic PAHs in the thylakoid membranes of algal cells (Marwood et al. 1999; Sargian et al. 2005). Early additions of inorganic nutrients to boost bacterial growth response and oil breakdown might be used to mitigate oil effects.

These experiments demonstrated not only negative effects of oil on ice biota but also the relevance of biological interactions in the outcome of exposure experiments. Both oil spill scenarios resulted in the inhibition of sea ice algal growth and EPS production. Ice algae are the base of an important Arctic food web, and EPS is a complex mixture of carbohydrates produced by algae that acts as a protectant within the ice. The varied responses of bacteria to oil exposure confirms that these microorganisms can quickly respond to oil exposure, but could potentially be limited in their growth potential by nutrient competition with ice algae.

Counterintuitively, Chl a levels did not substantially decrease after exposure of ice to oil, suggesting that the majority of cells were not necessarily destroyed by the oil but perhaps only inhibited. However, an abundance of apparently damaged cells suggests that these impacts may be long-lived. The striking differences in algal growth in control tanks between the first and second years can be attributed to methodological differences in tank inoculation and supplementation, highlighting the need to look at several components of the ice biota, including

bacteria and algae. In any case, it appears important, under a real oil spill scenario, to document the initial conditions when evaluating changes in abundances over time (e.g., growth rates) for both algae and bacteria. The observed differences in algal cell fluorescence properties should be further assessed as a tool to identify and detect effects of oil contamination in the field. More research is required to assess the consistent occurrence of these deviations for different taxa and evaluate whether this phenomenon results from intracellular damage.

Bacterial abundances appeared to respond not only to oil exposure but also to nutrient competition with sea ice algae. Here we suggest that bacterial response to oil might be greatest during the dark winter season with limited algal biomass and growth, while no abundance increase might occur after oil spills during the ice algal spring bloom.

Our study highlights the need for further investigations of oil exposure effects on diverse sea ice algal and bacterial communities. Such experiments might include interactions between light availability, algae, and bacteria to elucidate if oil-degrading bacteria might be more efficient biological cleanup agents in the absence of algal growth (i.e., in the absence of light) as our results suggest. The addition of inorganic nutrients might also increase the biodegradation by sea ice microbes. A wider range of algae should be tested, as algal diversity in our tanks was limited. Furthermore, we suggest studying the complete microbial network within such experiments, as bacterial loss terms could be important factors. Lower and varying oil concentrations should be utilized to study the biological response to sub-lethal oil concentrations. Clearly, future tank studies using the experimental and scientific insights gathered during this set of experiments can provide a solid scientific background to develop and improve adequate responses should an oil spill occur in Arctic waters.

STUDY PRODUCTS

Oggier M, Dilliplaine K (2014) Oil in Sea Ice: Implications of biota and microstructure. (Oral presentation) UAF Sea Ice Group, 10 January 2014, Fairbanks, AK.

Dilliplaine K, Oggier M (2014) Sea Ice Biology: Effects of biota on oil permeation in sea ice. (Poster presentation) Alaska Oil Spill Technology Symposium, 6–7 March 2014, Fairbanks, AK.

Oggier M (2014) X-Ray tomography to characterize entrapped oil in sea ice. (Poster presentation) International Conference on Porous Media, 27–30 May 2014, Milwaukee, WI.

Oggier M, Dilliplaine K (2014) Oil in Sea Ice: The story of 1 week in Barrow and 2 months in the lab. (Oral presentation) UAF Sea Ice Group, 11 July 2014, Fairbanks, AK.

Dilliplaine K, Oggier M, Eicken H, Bluhm B, Gradinger R, Collins RE (2015) Preliminary Findings of an Oil-in-Ice Mesocosm Experiment. (Poster presentation) Alaska Marine Science Symposium, 27 January 2015, Anchorage, AK.

Dilliplaine K, Oggier M, Eicken H, Bluhm B, Gradinger R, Collins RE (2016) Biological Influence and Impact of Sea Ice Biota in Ice-Covered Waters. (Oral presentation) Alaska Marine Science Symposium, 26 January 2016, Anchorage, AK.

Oggier M, Dilliplaine K, Eicken H, Bluhm B, Gradinger R, Collins RE (2016). Oil in ice: Evolution of pore space geometry occupied by crude oil. (Poster presentation) Alaska Marine Science Symposium, 26 January 2016, Anchorage, AK.

ACKNOWLEDGEMENTS

REFERENCES

Agusti S, Sánchez MC (2002) Cell variability in natural phytoplankton communities quantified by a membrane permeability probe. Limnol Ocean 47:818–828.

Aksmann A, Tukaj Z (2008) Intact anthracene inhibits photosynthesis in algal cells: A fluorescence induction study on *Chlamydomonas reinhardtii* cw92 strain. Chemosphere 74:26–32. doi:10.1016/j.chemosphere.2008.09.064

Alcoverro T, Conte E, Mazzella L (2000) Production of mucilage by the Adriatic epipelic diatom *Cylindrotheca closterium* (Bacillariophyceae) under nutrient limitation. J Phycol 36:1087–1095. doi:10.1046/j.1529-8817.2000.99193.x

AMAP (2010) Assessment 2007: Oil and Gas Activities in the Arctic - Effects and Potential Effects. Volume 2. Arctic Monitoring and Assessment Programme (AMAP), Oslo, Norway. vii + 277 pp.

Arar EJ, Collins GB (1997) Method 445.0 *In Vitro* Determination of Chlorophyll *a* and Pheophytin *a* in Marine and Freshwater Algae by Fluorescence. US Environmental Protection Agency, Washington, DC.

Arctic Council (2009) Arctic Marine Shipping Assessment 2009 Report. Arctic Council.

Aslam SN, Cresswell-Maynard T, Thomas DN, Underwood GJC (2012a) Production and characterization of the intra-and extracellular carbohydrates and polymeric substances (EPS) of three sea-ice diatom species, and evidence for a cryoprotective role for EPS. J Phycol 48:1494–1509. doi:10.1111/jpy.12004

Aslam SN, Underwood GJC, Kaartokallio H, Kaartokallio H, Norman L, Autio R, Fischer M, Kuosa H, Dieckmann GS, Thomas DN (2012) Dissolved extracellular polymeric substances (dEPS) dynamics and bacterial growth during sea ice formation in an ice tank study. Polar Biol 35:661–676. doi:10.1007/s00300-011-1112-0

Atlas RM, Horowitz A, Busdosh M (1978) Prudhoe crude oil in arctic marine ice, water, and sediment ecosystems: degradation and interactions with microbial and benthic communities. J Fish Res Board Canada 35:585–590. doi:10.1139/f78-104

Aumack CF, Juhl AR, Krembs C (2014) Diatom vertical migration within land-fast arctic sea ice. J Mar Syst 139:496–504. doi:10.1016/j.jmarsys.2014.08.013

Bassett C, Lavery AC, Maksym T, Wilkinson JP (2016) Broadband acoustic backscatter from crude oil under laboratory-grown sea ice. J Acoust Soc Am 140:2274–2287. doi:10.1121/1.4963876

Bates D, Mächler M, Bolker B, Walker S (2015) Fitting linear mixed-effects models using lme4. J Stat Softw 67(1):1–48. doi:10.18637/jss.v067.i01

Bitton G, Freihofer V (1978) Influence of extracellular polysaccharides on the toxicity of copper and cadmium toward *Klebsiella aerogenes*. Microb Ecol 4:119–125.

Bock C, Eicken H (2005) A magnetic resonance study of temperature-dependent microstructural evolution and self-diffusion of water in Arctic first-year sea ice. Ann Glaciol 40:179–184. doi:10.3189/172756405781813645

Boetius A, Albrecht S, Bakker K, Bienhold C., Felden J., Fernández-Méndez M., Hendricks S, Katlein C, Lalande C, Krumpen T, Nicolaus M, Peeken I, Rabe B, Rogacheva A, Rybakova E, Somavilla1 R, Wenzhöfer F, RV Polarstern ARK27-3-Shipboard Science Party (2013) Export of algal biomass from the melting Arctic Sea ice. Science 339(6126):1430–1432. doi:10.1126/science.1231346

Bragg JR, Prince RC, Harner EJ, Atlas RM (1994) Effectiveness of bioremediation for the *Exxon Valdez* oil spill. Nature 368:413–418. doi:10.1038/367532a0

Brakstad OG, Nonstad I (2008) Responses of microbial communities in Arctic sea ice after contamination by crude petroleum oil. Microb Ecol 55:540–552. doi:10.1007/s00248-007-9299-x

Buist I, Potter S, Nedwed T, Mullin J (2011) Herding surfactants to contract and thicken oil spills in pack ice for *in situ* burning. Cold Reg Sci Technol 67:3–23. doi:10.1016/j.coldregions.2011.02.004

Buist IA, Dickins DF (1987) Experimental spills of crude oil in pack ice. Int Oil Spill Conf Proc 1987:373–381. doi:10.7901/2169-3358-1987-1-373

Chen J (2014) Factors affecting carbohydrate production and the formation of transparent exopolymer particles (TEP) by diatoms. Ph.D. Thesis, Texas A&M University.

Cohn SA, Farrell JF, Munro JD, Ragland RL, Weitzell Jr. RE, Wibisono BL (2003) The effect of temperature and mixed species composition on diatom motility and adhesion. Diatom Res 18:225–243. doi:10.1080/0269249X.2003.9705589

Cole DM, Shapiro LH (1998) Observations of brine drainage networks and microstructure of first-year sea ice. J Geophys Res Ocean 103:21179–21750. doi:10.1029/98JC01264

Collins R, Rocap G, Deming JW (2010) Persistence of bacterial and archaeal communities in sea ice through an Arctic winter. Environ Microbiol 12:1828–1841. doi:10.1111/j.1462-2920.2010.02179.x

Cota GF, Legendre L, Gosselin M, Ingram RG (1991) Ecology of bottom ice algae: I. Environmental controls and variability. J Mar Syst 2:257–277. doi:10.1016/0924-7963(91)90036-T

Cota GF, Smith REH (1991) Ecology of bottom ice algae: II. Dynamics, distributions and productivity. J Mar Syst 2:279–295. doi:10.1016/0924-7963(91)90037-U

Cox GFN, Weeks WF (1975) Brine drainage and initial salt entrapment in sodium chloride ice. CRREL Research Report 345. US Department of Defense, Army Corps of Engineers, Cold Regions Research and Engineering Laboratory, Hanover, NH.

Cox GFN, Weeks WF (1983) Equations for determining the gas and brine volumes in sea-ice samples. J Glaciol 29:306–316. doi:10.3198/1983JoG29-102-306-316

Cross WE (1987) Effects of oil and chemically treated oil on primary productivity of high arctic ice algae studied *in situ*. Arctic 40:266–276.

Cross WE, Martin CM (1987a) Effects of oil and chemically treated oil on nearshore under-ice meiofauna studied *in situ*. Arctic 40:258–265.

Cullen JJ, Geider RJ, Ishizaka J, Kiefer DA, Marra J, Sakshaug E, Raven JA (1993) Towards a general description of phytoplankton growth for biogeochemical models. In: Evans GT, Fasham MJR (Eds), Towards a Model of Ocean Biogeochemical Processes. NATO ASI Series (Series I: Global Environmental Change), Vol 10. Springer, Berlin, Germany.

Decker CJ, Fleeger JW (1984) The effect of crude oil on the colonization of meiofauna into salt marsh sediments. Hydrobiologia 118:49–58.

Delille D (2000) Response of antarctic soil bacterial assemblages to contamination by diesel fuel and crude oil. Microb Ecol 40:159–168. doi:10.1007/s002480000027

Delille D, Bassères A, Dessommes A (1997) Seasonal variation of bacteria in sea ice contaminated by diesel fuel and dispersed crude oil. Microb Ecol 33:97–105. doi:10.1007/s002489900012

Delille D, Bassères A, Dessommes A (1998) Effectiveness of bioremediation for oil-polluted antarctic seawater. Polar Biol 19:237–241. doi:10.1007/s003000050240

Dickins D, Brandvik PJ, Bradford J, Faksness LG, Liberty L, Daniloff R (2008) Svalbard 2006 experimental oil spill under ice: remote sensing, oil weathering under arctic conditions and assessment of oil removal by *in situ* burning. Int Oil Spill Conf Proc. Vol 2008-1:681–688. doi:10.7901/2169-3358-2008-1-681

Dickins D, Brandvik PJ, Faksness L-G, Bradford J, Liberty L (2006) 2006 Svalbard experimental spill to study spill detection and oil behavior in ice. Final Technical Report (contract number 1435-0106-CT-3925). US Department of Interior, Minerals Management Service, Herndon, VA.

Dickins D, DF Dickins Associates LLC, Fleet Technology Ltd (1992) Behaviour of Spilled Oil at Sea (BOSS): Oil-in-Ice Fate and Behaviour. Report prepared for Environment Canada, US Minerals Management Service, and American Petroleum Institute. 200 pp.

Dickins D, DF Dickins Associates LLC (2011) Behavior of oil spills in ice and implications for arctic spill response. In: Proceedings of the Arctic Technology Conference, 7–9 February 2011, Houston, TX.

DuBois M, Gilles KA, Hamilton JK, Rebers PA, Smith F (1956) Colorimetric method for determination of sugars and related substances. Anal Chem 28:350–356. doi:10.1021/ac60111a017

Durbin EG, Casas MC (2014) Early reproduction by *Calanus glacialis* in the Northern Bering Sea: The role of ice algae as revealed by molecular analysis. J Plankton Res 36:523–541. doi:10.1093/plankt/fbt121

Echeveste P, Agustí S, Dachs J (2010) Cell size dependent toxicity thresholds of polycyclic aromatic hydrocarbons to natural and cultured phytoplankton populations. Environ Pollut 158:299–307. doi:10.1016/j.envpol.2009.07.006

Eicken H (2003) From the microscopic, to the macroscopic, to the regional scale: growth, microstructure and properties of sea ice. In: Thomas D, Dickemann GS (Eds), Sea Ice: An Introduction to Its Physics, Chemistry, and Geology. Blackwell Science, London, England. pp. 22–81.

Eicken H, Bock C, Wittig R, Miller H, Poertner H-O (2000) Magnetic resonance imaging of sea-ice pore fluids: methods and thermal evolution of pore microstructure. Cold Reg Sci Technol. 31-3:207–225. doi:10.1016/S0165-232X(00)00016-1

Elarbaoui S, Richard M, Boufahja F, Mahmoudi E, Thomas-Guyon H (2015) Effect of crude oil exposure and dispersant application on meiofauna: an intertidal mesocosm experiment. Environ Sci Process Impacts 17:997–1004. doi:10.1039/C5EM00051C

Farmer D, Li M (1994) Oil dispersion by turbulence and coherent circulations. Ocean Eng 21:575–586. doi:10.1016/0029-8018(94)90007-8

Fiala M, Delille D (1999) Annual changes of microalgae biomass in Antarctic sea ice contaminated by crude oil and diesel fuel. Polar Biol 21:391–396. doi:10.1007/s003000050378

Fingas MF, Hollebone BP (2003) Review of behaviour of oil in freezing environments. Mar Pollut Bull 47:333–340. doi:10.1016/S0025-326X(03)00210-8

Folke C, Carpenter SR, Walker B, Scheffer M, Elmqvist T, Gunderson L, Holling CS (2004) Regime shifts, resilience, and biodiversity in ecosystem management. Annu Rev Ecol Evol Syst 35:557–581. doi:10.2307/annurev.ecolsys.35.021103.30000021

Galley RY, Else BGT, Geilfus N, Hare AA, Isleifson D, Barber DG, Rysgaard S (2015) Imaged brine inclusions in young sea ice: Shape, distribution, and formation timing. Cold Reg Sci Technol 111:39–48. doi:10.1016/j.coldregions.2014.12.011

Gardiner WW, Word JQ, Word JD, Perkisn RA, McFarlin KM, Hester BW, Word LS, Ray CM (2013) The acute toxicity of chemically and physically dispersed crude oil to key Arctic species under Arctic conditions during the open water season. Environ Toxicol Chem 32:2284–300. doi:10.1002/etc.2307

Garrisson D, Buck K (1989) The biota of Antarctic pack ice in the Weddell Sea and Antarctic Peninsula regions. Polar Biol 10:211–219.

Gautier DL, Bird KJ, Charpentier RR, Grantz A, Houseknecht DW, Klett TR, Moore TE, Pitman JK, Schenk CJ, Schuenemeyer JH, Sorenson K, Tennyson ME, Valin ZC, Wandrey CJ (2009) Assessment of undiscovered oil and gas in the Arctic. Science 324:1175–1179. doi:10.1126/science.1169467

Gerdes B, Brinkmeyer R, Dieckmann G, Helmke E (2005) Influence of crude oil on changes of bacterial communities in Arctic sea-ice. FEMS Microbiol Ecol 53:129–139. doi:10.1016/j.femsec.2004.11.010

Gilde K, Pinckney JL (2012) Sublethal Effects of crude oil on the community structure of estuarine phytoplankton. Estuar Coasts 35:853–861. doi:10.1007/s12237-011-9473-8

Glaeser JL, Vance GP (1972) A study of the behavior of oil spills in the arctic. Offshore Technology Conference, 1–3 May 1972, Houston, TX. doi:10.4043/1551-MS

Golden KM (2009) Climate change and the mathematics of transport in sea ice. Not Am Math Soc 56:562–584.

Gosselin M, Legendre L (1990) Light and nutrient limitation of sea-ice microalgae (Hudson Bay, Canadian Arctic). J Phycol 37:1125.

Gosselin M, Levasseur M, Wheeler PA, Horner RA, Booth BC (1997) New measurements of phytoplankton and ice algal production in the Arctic Ocean. Deep Res Part II Top Stud Oceanogr 44:1623–1644. doi:10.1016/S0967-0645(97)00054-4

Gradinger R (1999) Vertical fine structure of the biomass and composition of algal communities in Arctic pack ice. Mar Biol 133:745–754. doi:10.1007/s002270050516

Gradinger R, Friedrich C, Spindler M (1999) Abundance, biomass and composition of the sea ice biota of the Greenland Sea pack ice. Deep Sea Res Part II Top Stud Oceanogr 46:1457–1472. doi:10.1016/S0967-0645(99)00030-2

Gradinger R, Ikävalko J (1998) Organism incorporation into newly forming Arctic sea ice in the Greenland Sea. J Plankton Res 20:871–886. doi:10.1093/plankt/20.5.871

Gradinger R, Kaufman M, Bluhm B (2009) Pivotal role of sea ice sediments in the seasonal development of near-shore Arctic fast ice biota. Mar Ecol Prog Ser 394:49–63. doi:10.3354/meps08320

Gradinger R, Zhang Q (1997) Vertical distribution of bacteria in Arctic sea ice from the Barents and Laptev Seas. Polar Biol 17:448–454. doi:10.1007/s003000050139

Haecky P, Jonsson S, Andersson A (1998) Influence of sea ice on the composition of the spring phytoplankton bloom in the northern Baltic Sea. Polar Biol 20:1–8. doi:10.1007/s003000050270

Harsem Ø, Heen K, Rodrigues JMP, Vassdal T (2013) Oil exploration and sea ice projections in the Arctic. Polar Rec (Gr Brit) 51:91–106. doi:10.1017/S0032247413000624

Hjorth M, Nielsen TG (2011) Oil exposure in a warmer arctic: potential impacts on key zooplankton species. Mar Biol 158:1339–1347. doi:10.1007/s00227-011-1653-3

Horner R, Schrader GC (1982) Relative contributions of ice algae, phytoplankton, and benthic microalgae to primary production in nearshore regions of the Beaufort Sea. Arctic 35:485–503. doi:10.14430/arctic2356

Hsiao SC (1978) Effects of crude oils on the growth of Arctic marine phytoplankton. Environ Pollut 17:93–107.

Hsiao SIC (1980) Quantitative composition, distribution, community structure and standing stock of sea ice microalgae in the Canadian Arctic. Arctic 33:768–793. doi:10.14430/arctic2595

ITOPF (2011) Fate of marine oil spills. Technical Information Paper 2. International Tanker Owners Pollution Federation , London, England. http://www.itopf.com/knowledge-resources/documents-guides/document/tip-2-fate-of-marine-oil-spills/

Jiang Z, Huang Y, Xu X, Liao Y, Shou L, Jingjing L, Quanzhen C, Zeng J (2010) Advance in the toxic effects of petroleum water accommodated fraction on marine plankton. Acta Ecol Sin 30:8–15. doi:10.1016/j.chnaes.2009.12.002

Jin M, Deal C, Wang J, Alexander V, Gradinger R, Saitoh S, Iida T, Wan Z, Stabeno P (2007) Ice-associated phytoplankton blooms in the southeastern Bering Sea. Geophys Res Lett 34:1–6. doi:10.1029/2006GL028849

Karlsson J (2009) A laboratory study of fixation, release rates and small scale movement of oil. MS Thesis, University of Copenhagen.

Karlsson J, Petrich C, Eicken H (2011) Oil entrainment and migration in laboratory-grown saltwater ice. In: Proceedings of the 21st International Conference on Port and Ocean Engineering under Arctic Conditions. POAC11, Montreal, Canada.

Krembs C, Eicken H, Deming JW (2011) Exopolymer alteration of physical properties of sea ice and implications for ice habitability and biogeochemistry in a warmer Arctic. Proc Natl Acad Sci USA 108:3653–3658. doi:10.1073/pnas.1100701108

Krembs C, Eicken H, Junge K, Deming JW (2002) High concentrations of exopolymeric substances in Arctic winter sea ice: Implications for the polar ocean carbon cycle and cryoprotection of diatoms. Deep Res Part I Oceanogr Res Pap 49:2163–2181. doi:10.1016/S0967-0637(02)00122-X

Krembs C, Engel A (2001) Abundance and variability of microorganisms and transparent exopolymer particles across the ice-water interface of melting first-year sea ice in the Laptev Sea (Arctic). Mar Biol 138:173–185. doi:10.1007/s002270000396

Krembs C, Gradinger R, Spindler M (2000) Implications of brine channel geometry and surface area for the interaction of sympagic organisms in Arctic sea ice. J Exp Mar Bio Ecol 243:55–80. doi:10.1016/S0022-0981(99)00111-2

Krembs C, Mock T, Gradinger R (2001) A mesocosm study of physical-biological interactions in artificial sea ice: Effects of brine channel surface evolution and brine movement on algal biomass. Polar Biol 24:356–364. doi:10.1007/s003000000219

Kuparinen J, Autio R, Kaartokallio H (2011) Sea ice bacterial growth rate, growth efficiency and preference for inorganic nitrogen sources in the Baltic Sea. Polar Biol 34:1361–1373. doi:10.1007/s00300-011-0989-y

Lake RA, Lewis EL (1970) Salt rejection by sea ice during growth. J Geophys Res 75:583–597. doi:10.1029/JC075i003p00583

Lange BA, Michel C, Beckers JF, Casey A, Flores H, Hatam I, Meisterhans G, Niemi A, Haas C (2015) Comparing springtime ice-algal chlorophyll *a* and physical properties of multi-year and first-year sea ice from the Lincoln Sea. PLoS One 10(4). doi:10.1371/journal.pone.0122418

Lee SH, Whitledge TE, Kang SH (2008) Spring time production of bottom ice algae in the landfast sea ice zone at Barrow, Alaska. J Exp Mar Bio Ecol 367:204–212. doi:10.1016/j.jembe.2008.09.018

Leppäranta M, Manninen T (1988) The brine and gas content of sea ice with attention to low salinities and high temperatures. Finnish Inst Mar Res Intern Rep. 2:1–14.

Li M, Garrett C (1998) The relationship between oil droplet size and upper ocean turbulence. Mar Pollut Bull 36:961–970. doi:10.1016/S0025-326X(98)00096-4

Liu SB, Chen XL, He HL, Zhang XY, Xie BB, Yu Y, Chen B, Zhou BC, Zhang YZ (2013) Structure and ecological roles of a novel exopolysaccharide from the Arctic sea ice bacterium *Pseudoalteromonas* sp. strain SM20310. Appl Environ Microbiol 79:224–230. doi:10.1128/AEM.01801-12

MacNeill MR, Goodman RH (1987) Oil motion during lead closure. Environmental Studies Revolving Funds Report 053. Ottawa, Canada. 13 pp.

Mahoney A, Eicken H, Gaylord AG, Shapiro L (2007) Alaska landfast sea ice: Links with bathymetry and atmospheric circulation. J Geophys Res Ocean 112:1–18. doi:10.1029/2006JC003559

Malmgren F (1927) On the properties of sea-ice. In: Sverdrup HU (Ed), The Norwegian North Polar Expedition with the 'Maud' 1918 – 1925, Vol 1a:1–67. John Griegs Boktrykkeri, Bergen, Norway.

Manes SS, Gradinger R (2009) Small scale vertical gradients of Arctic ice algal photophysiological properties. Photosynth Res 102:53–66. doi:10.1007/s11120-009-9489-0

Margesin R, Schinner F (1999) Biological decontamination of oil spills in cold environments. J Chem Technol Biotechnol 74:381–389. doi:10.1002/(SICI)1097-4660(199905)74:5<381::AID-JCTB59>3.0.CO;2-0

Martin S (1979) A field study of brine drainage and oil entrainment in first-year sea ice. Deep Sea Res Part B Oceanogr Lit Rev 22:473–502. doi:10.1016/0198-0254(80)95767-2

Martín-Robichaud D, Peterson RH (1998) Effects of light intensity, tank colour and photoperiod on swimbladder inflation success in larval striped bass, *Morone saxatilis* (Walbaum). Aquac Res 29:539–547. doi:10.1046/j.1365-2109.1998.00234.x

Marwood CA, Smith RE, Solomon KR, Charlton MN, Greenberg BM (1999) Intact and photomodified polycyclic aromatic hydrocarbons inhibit photosynthesis in natural assemblages of Lake Erie phytoplankton exposed to solar radiation. Ecotoxicol Environ Saf 44:322–327. doi:10.1006/eesa.1999.1840

Masutani SM, Adams EE (2001) Experimental study of multi-phase plums with application to deep ocean oil spills. Final Technical Report (contract number 1435-0198-CT-30964). US Department of Interior, Minerals Management Service, Herndon, VA.

Maus S, Becker J, Leisinger S, Matzl M, Schneebeli M, Wiegmann A (2015) Oil saturation of the sea ice pore space. In: Proceedings of the 23st International Conference on Port and Ocean Engineering under Arctic Conditions. POAC 2015, Trondheim, Norway.

Maus S, Leisinger S, Matzl M, Schneebeli M, Wiegmann A (2013) Modelling oil entrapment in sea ice on the basis of 3D micro-tomographic images. In: Proceedings 22nd International Conference on Port and Ocean Engineering under Arctic Conditions. POAC13, Espoo, Finland.

McConnell B, Gradinger R, Iken K, Bluhm B (2012) Growth rates of arctic juvenile *Scolelepis squamata* (Polychaeta: Spionidae) isolated from Chukchi Sea fast ice. Polar Biol 35:1487–1494. doi:10.1007/s00300-012-1187-2

Michel C, Ingram RG, Harris LR (2006) Variability in oceanographic and ecological processes in the Canadian Arctic Archipelago. Prog Oceanogr 71:379–401. doi:10.1016/j.pocean.2006.09.006

Mock T, Dieckmann GS, Haas C, Krell A, Tison JL, Belem A, Papadimitriou S, Thomas ND (2002) Micro-optodes in sea ice: A new approach to investigate oxygen dynamics during sea ice formation. Aquat Microb Ecol 29:297–306. doi:10.3354/ame029297

Mock T, Gradinger R (1999) Determination of Arctic ice algal production with a new *in situ* incubation technique. Mar Ecol Prog Ser 177:15–26. doi:10.3354/Meps177015

Mundy CJ, Barber DG, Michel C (2005) Variability of snow and ice thermal, physical and optical properties pertinent to sea ice algae biomass during spring. J Mar Syst 58:107–120. doi:10.1016/j.jmarsys.2005.07.003

Nakawo M, Sinha NK (1981) Growth rate and salinity profile of first-year sea ice in the high Arctic. J Glaciol 27:313–328.

Nichols CM, Bowman JP, Guezennec J (2005) Effects of incubation temperature on growth and production of exopolysaccharides by an antarctic sea ice bacterium grown in batch culture. Appl Environ Microbiol 71:3519–3523. doi:10.1128/AEM.71.7.3519

NORCOR (1975) The interaction of crude oil with Arctic sea ice. Beaufort Sea Project Technical Report No. 27. Department of the Environment, Victoria, Canada.

Otsuka N, Kondo H, Saeki H (2004) Experimental study on the characteristics of oil ice sandwich. Proceedings of Oceans '04 Vol 3:1470–1475. doi:10.1109/OCEANS.2004.1406337

Overland JE, Wang M (2013) When will the summer Arctic be nearly sea ice free? Geophys Res Lett 40:2097–2101. doi:10.1002/grl.50316

Özhan K, Miles SM, Gao H, Bargu S (2014) Relative phytoplankton growth responses to physically and chemically dispersed South Louisiana sweet crude oil. Environ Monit Assess 186:3941–3956. doi:10.1007/s10661-014-3670-4

Ozturk S, Aslim B (2010) Modification of exopolysaccharide composition and production by three cyanobacterial isolates under salt stress. Environ Sci Pollut Res 17:595–602. doi:10.1007/s11356-009-0233-2

Perez P, Fernandez E, Beiras R (2010) Fuel toxicity on *Isochrysis galbana* and a coastal phytoplankton assemblage: Growth rate vs. variable fluorescence. Ecotoxicol Environ Saf 73:254–261. doi:10.1016/j.ecoenv.2009.11.010

Perovich DK, Richter-Menge JA (1994) Surface characteristics of lead ice. J Geophys Res 99:16341–16350. doi:10.1029/94JC01194

Petrich C, Karlsson J, Eicken H (2013) Porosity of growing sea ice and potential for oil entrainment. Cold Reg Sci Technol 87:27–32. doi:10.1016/j.coldregions.2012.12.002

Porter KG, Feig YS (1980) The use of DAPI for identifying aquatic microfloral. Limnol Oceanogr 25:943–948. doi:10.4319/lo.1980.25.5.0943

Poulin M, Daugbjerg N, Gradinger R, Ilyash L, Ratkova T, von Quillfeldt C (2011) The pan-Arctic biodiversity of marine pelagic and sea-ice unicellular eukaryotes: A first-attempt assessment. Mar Biodivers 41:13–28. doi:10.1007/s12526-010-0058-8

Prince RC, Coolbaugh TS, Parkerton TF (2016) Oil dispersants do facilitate biodegradation of spilled oil. Proc Natl Acad Sci USA 113(11):142. doi:10.1073/pnas.1525333113

Pringle DJ, Miner JE, Eicken H, Golden KM (2009) Pore space percolation in sea ice single crystals. J Geophys Res Ocean 114:C12017. doi:10.1029/2008JC005145

Pringle DJ, Trodahl HJ, Haskell TG (2006) Direct measurement of sea ice thermal conductivity: No surface reduction. J Geophys Res Ocean 111:C5. doi:10.1029/2005JC002990

Ralph PJ, Ryan KG, Martin A, Fenton G (2007) Melting out of sea ice causes greater photosynthetic stress in algae than freezing in. J Phycol 43:948–956. doi:10.1111/j.1529-8817.2007.00382.x

Ratkova TN, Wassmann P (2005) Sea ice algae in the White and Barents seas: Composition and origin. Polar Res 24:95–110. doi:10.1111/j.1751-8369.2005.tb00143.x

Reimnitz E, Clayton JR, Kempema EW, Payne JR, Weber WS (1993) Interaction of rising frazil with suspended particles: tank experiments with applications to nature. Cold Reg Sci Technol 21:117–135. doi:10.1016/0165-232X(93)90002-P

Riedel A, Michel C, Gosselin M (2006) Seasonal study of sea-ice exopolymeric substances on the Mackenzie shelf: Implications for transport of sea-ice bacteria and algae. Aquat Microb Ecol 45:195–206. doi:10.3354/ame045195

Roth BL, Poot M, Yue ST, Millard PJ (1997) Bacterial viability and antibiotic susceptibility testing with SYTOX green nucleic acid stain . Appl Environ Microbiol 63:2421–2431.

Salomon ML, Maus S, Arntsen M, O'Sadnick M, Petrich C, Wilde F (2016) Distribution of oil in sea ice: Laboratory experiments for 3-dimensional microCT investigations. In: Proceedings of the 26th International Ocean and Polar Engineering Conference, 26 June–1 July 2016, Rhodes, Greece. Vol 3:1328–1334. International Society of Offshore and Polar Engineers, Cupertino, CA.

Sargian P, Mostajir B, Chatila K, Ferreyra, GA, Pelletier E, Demers S (2005) Non-synergistic effects of water-soluble crude oil and enhanced ultraviolet-B radiation on a natural plankton assemblage. Mar Ecol Prog Ser 294:63–77. doi:10.3354/meps294063

Selldén G, Leech RM (1981) Localization of DNA in mature and young wheat chloroplasts using the fluorescent probe 4'-6-diamidino-2-phenylindole. Plant Physiol 68:731–734. doi:10.1104/pp.68.3.731

Singer MM, Aurand D, Bragin GE, Clark JR, Coelho GM, Sowby ML, Tjeerdema RS (2000) Standardization of the preparation and quantitation of water-accommodated fractions of petroleum for toxicity testing. Mar Pollut Bull 40:1007–1016. doi:10.1016/S0025-326X(00)00045-X

Singh AK, Gaur JP (1988) Effect of Assam crude on photosynthesis and associated electron transport system in *Anabaena doliolum*. Bull Environ Contam Toxicol 41:776–780. doi:10.1007/BF02021033

Siron R, Pelletier E, Delille D, Roy S (1993) Fate and effects of dispersed crude oil under icy conditions simulated in mesocosms. Mar Environ Res 35:273–302. doi:10.1016/0141-1136(93)90098-K

Smedsrud Henrik LH (2001) Frazil-ice entrainment of sediment: Large-tank laboratory experiments. J Glaciol 47:461–471. doi:10.3189/172756501781832142

SOKI Wiki (2014) Carbohydrate Analysis-Methods-Confluence, SOKI, Antarctic Climate and Ecosystems Co-operative Research Centre. http://www.soki.aq/display/StandMeth/Carbohydrate+Analysis

Søreide JE, Leu E, Berge J, Graeve M, Falk-Petersen S (2010) Timing of blooms, algal food quality and *Calanus glacialis* reproduction and growth in a changing Arctic. Glob Chang Biol 16:3154–3163. doi:10.1111/j.1365-2486.2010.02175.x

Suzuki Y, Kudoh S, Takahashi M (1997) Photosynthetic and respiratory characteristics of an Arctic ice algal community living in low light and low temperature conditions. J Mar Syst 11:111–121. doi:10.1016/S0924-7963(96)00032-2

Szymanski A, Gradinger R (2016) The diversity, abundance and fate of ice algae and phytoplankton in the Bering Sea. Polar Biol 39:309–325. doi:10.1007/s00300-015-1783-z

Thingstad TF, Lignell R (1997) Theoretical models for the control of bacterial growth rate, abundance, diversity and carbon demand. Aquat Microb Ecol 13:19–27. doi:10.3354/ame013019

Tkalich P, Chan ES (2002) Vertical mixing of oil droplets by breaking waves. Mar Pollut Bull 44:1219–1229. doi:10.1016/S0025-326X(02)00178-9

van der Merwe P, Lannuzel D, Nichols CAM, Meiners K, Heil P, Norman L, Thams DN, Bowie AR (2009) Biogeochemical observations during the winter-spring transition in East Antarctic sea ice: Evidence of iron and exopolysaccharide controls. Mar Chem 115:163–175. doi:10.1016/j.marchem.2009.08.001

Veldhuis M, Kraay G, Timmermans K (2001) Cell death in phytoplankton: correlation between changes in membrane permeability, photosynthetic activity, pigmentation and growth. Eur J Phycol 36:167–177. doi:10.1080/09670260110001735318

Vézina AF, Demers S, Laurion I, Sime-Ngando T, Juniper SK, Devine L (1997) Carbon flows through the microbial food web of first-year ice in resolute passage (Canadian High Arctic). J Mar Syst 11:173–189. doi:10.1016/S0924-7963(96)00037-1

Weeks W (2010) On sea ice. University of Alaska Press, Fairbanks, AK.

Weissenberger J (1998) Arctic Sea ice biota: Design and evaluation of a mesocosm experiment. Polar Biol 19:151–159. doi:10.1007/s003000050228

Weissenberger J, Dieckmann G, Gradinger R, Spindler M (1992) Sea ice: A cast technique to examine and analyze brine pockets and channel structure. Limnol Oceanogr 37:179–183. doi:10.4319/lo.1992.37.1.0179

Weissenberger J, Grossmann S (1998) Experimental formation of sea ice: Importance of water circulation and wave action for incorporation of phytoplankton and bacteria. Polar Biol 20:178–188. doi:10.1007/s003000050294

Williamson DH, Fennell DJ (1979) [62] Visualization of yeast mitochondrial DNA with the fluorescent stain "DAPI." Methods Enzymol 56:728–733. doi:10.1016/0076-6879(79)56065-0

Wolfe LS, Hoult DP (1974) Effects of oil under sea ice. J Glaciol 13:473–488.

Zhang Q, Gradinger R, Spindler M (1999) Experimental study on the effect of salinity on growth rates of Arctic-sea-ice algae from the Greenland Sea. Boreal Environ Res 4:1–8.

Zheng L, Yapa PD (2000) Buoyant velocity of spherical and nonspherical bubbles/droplets. J Hydraul Eng 126:852–854. doi:10.1061/(ASCE)0733-9429(2000)126:11(852)

Zhou J, Delille B, Kaartokallio H, Kattner G, Kuosa H, Tison J-L, Autio R, Dieckmann GS, Evers K-U, Jorgensen, L, Kennedy H, Kotovitch M, Luhtanen A-M, Stedmon CA, Thomas DN (2014) Physical and bacterial controls on inorganic nutrients and dissolved organic carbon during a sea ice growth and decay experiment. Mar Chem 166:59–69. doi:10.1016/j.marchem.2014.09.013

Zubov, NN (1943) Arctic Ice (English translation). US Navy Electronics Laboratory, San Diego, CA. 491 p.

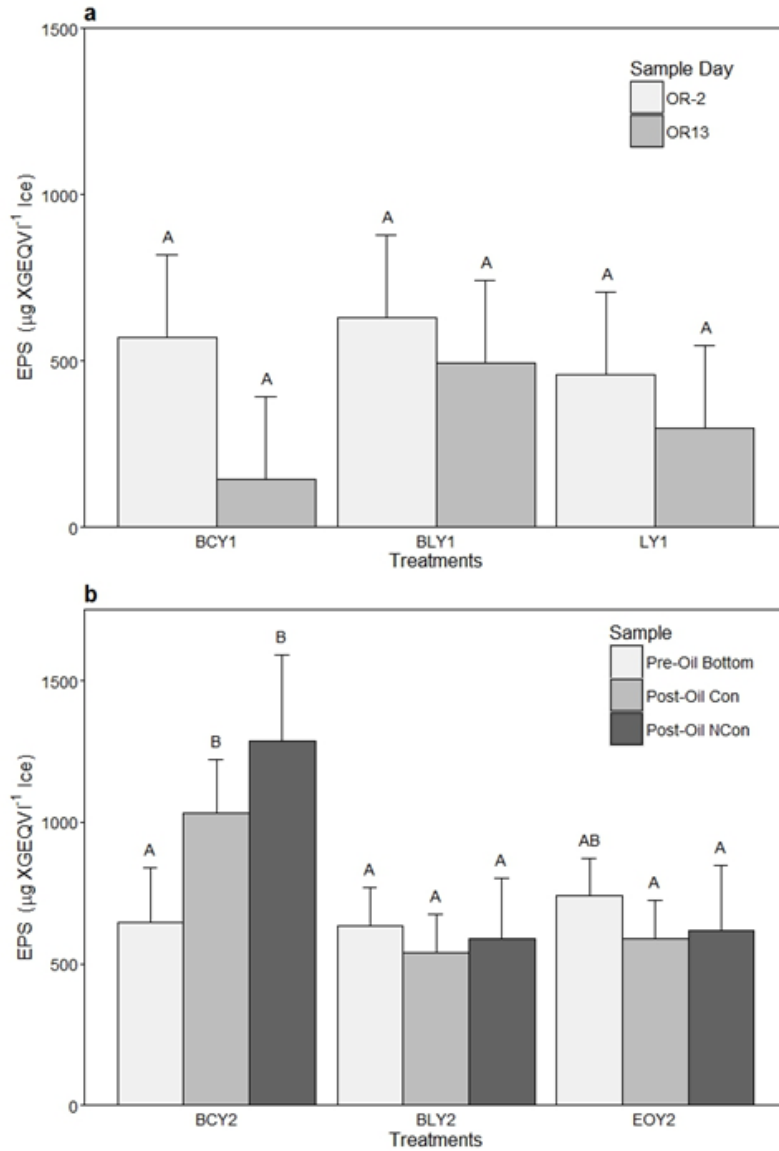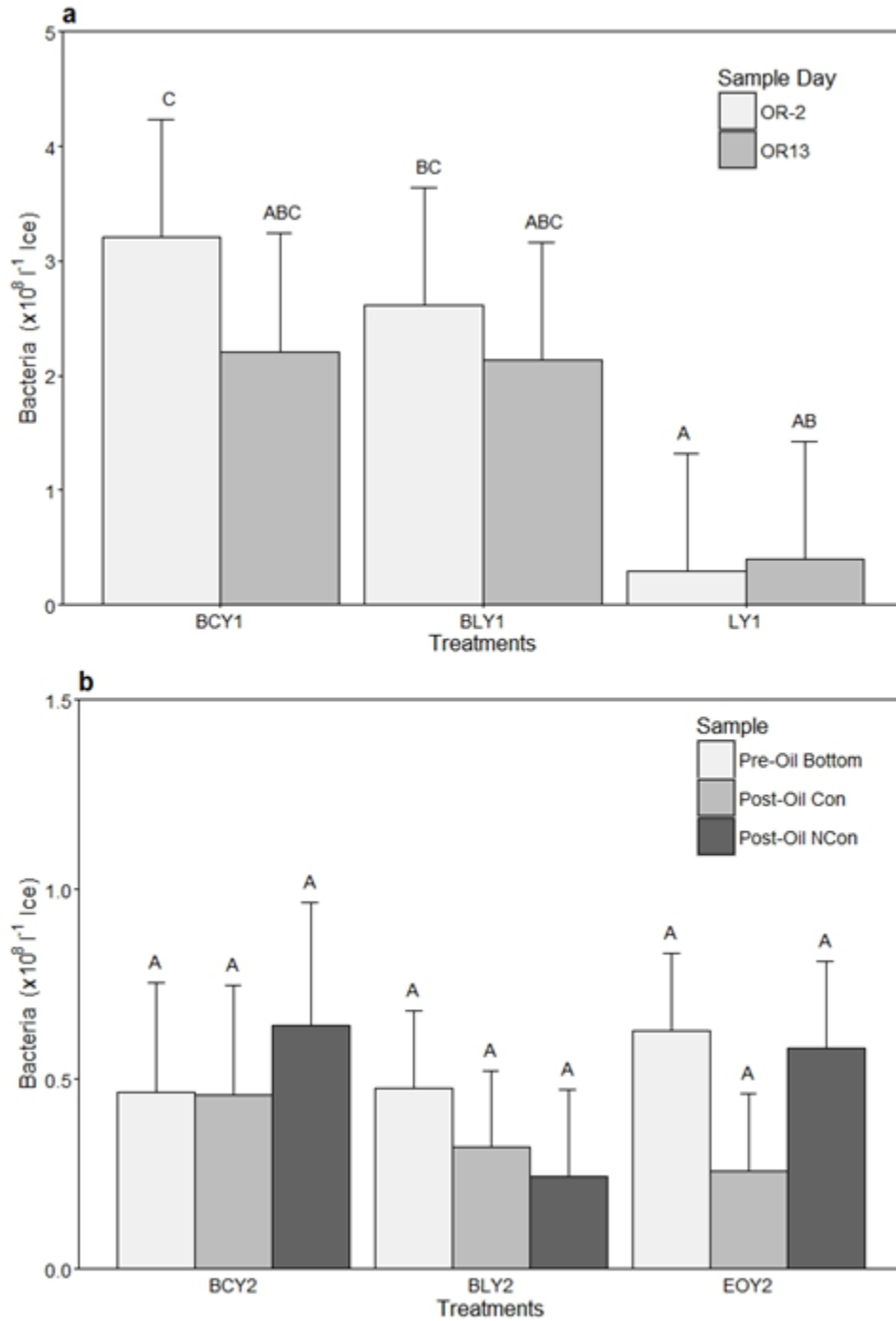APPENDICES

List of Appendix Figures

List of Appendix Tables

Appendix Figure 1. Mean extracellular polymeric substances (EPS) concentrations in (a) Y1 full ice cores and (b) Y2 bottom ice sections. Conservative (Con) and Non-Conservative (Sections) are represented. Error bars represent the 95% confidence interval. Letters above error bars represent Tukey's post hoc group assignment.

Appendix Figure 2. Mean bacteria abundance in mean extracellular polymeric substances (EPS) concentrations in (a) Y1 full ice cores and (b) Y2 bottom ice sections. Conservative (Con) and Non-Conservative (Sections) are represented. Error bars represent the 95% confidence interval. Letters above error bars represent Tukey's post hoc group assignment.
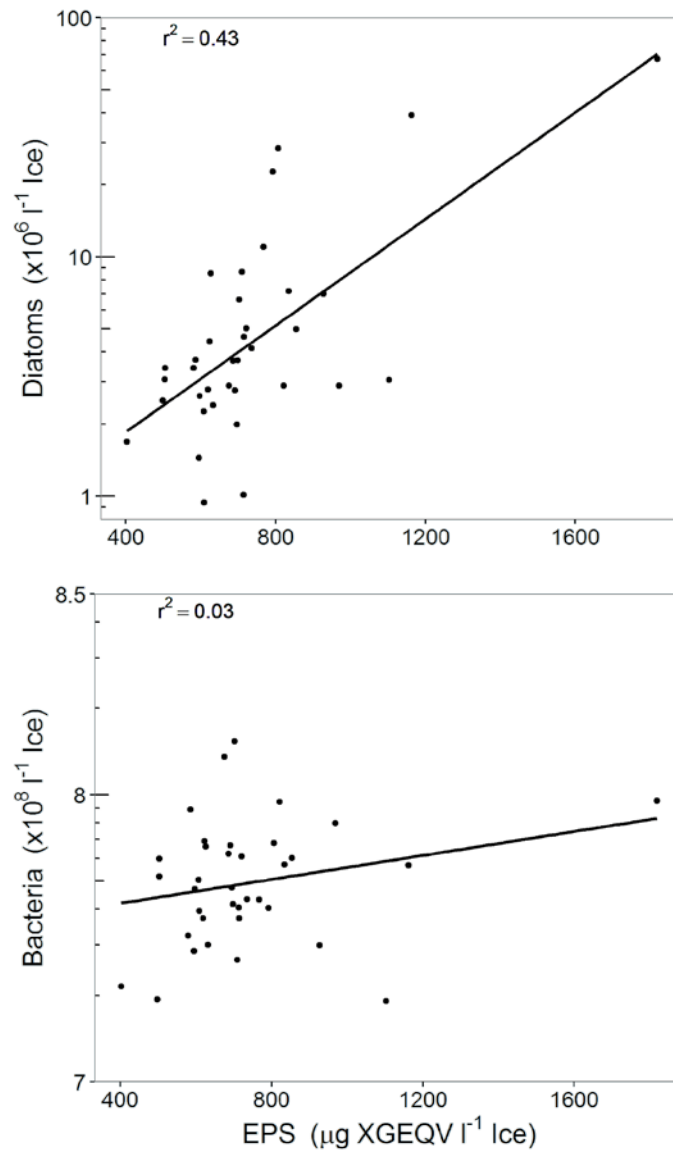
Appendix Figure 3. Regression analysis of diatom and bacterial abundance with EPS; recorded in μg Xanthum Gum Equivalents (XGEQV). Sections from oiled tanks at OR+10 are not included. Adjusted r^2 values are reported.

Appendix Table 1. Summary of tank, equipment, oil and treatment set-up and differences between 2014 (Y1) and 2015 (Y2). Acronyms: Biological Control Year 1 (BCY1), Biological Lens Year 1 (BLY1), Oil Lens Year 1 (LY1), Biological Control Year 2 (BCY2), Biological Lens Year 2 (BLY2), Emulsified Oil Year 2 (EOY2), Emulsified Oil 2 (EOII), Alaska North Slope crude oil (ANS). na= not applicable (not collected).

YEAR		Y1 (2014)	Y2 (2015)
TREATMENTS		BCY1	BCY2
		BLY1	BLY2
		LY1	EOY2
			EOII
OIL	Type	ANS Crude Oil	ANS Crude Oil
	Volume	7 liters	2 liters: BLY2
			0.5 liters: EOY2, EOII
	Releases	1	2
HEAT	Power (watts)	150	3 x 10, 1 x 15
	Control	Variable Control	On/Off
NUTRIENTS	Nutrient Addition	No	Yes
	Type	na	F/10
	Inner Wall Color	White	Black
	Starting Salinity	30	26
	Core Sectioning	Variable	Conservative
	Genomics	No	Yes
			Under ice slurry and density
	Inoculation Method	Surface Entrainment	layering
	Sample Size	n=6	n=3 BCY2; n=6 BLY2, EOY2, EOII

Appendix Table 2. Experimental timelines in 2014 (Y1) and 2015 (Y2) with respect to Oil Release (OR) and day of experiment. Acronyms: Oil Release (OR), Oil Release 2 (ORII), minus symbol (-) indicates days prior to oil release, plus sign (+) indicates days post oil release.

	Event	Y1 Relation to OR	Y1 Day of Experiment	Y2 Relation to OR	Y2 Day of Experiment
Main Experiment	Field Collections	OR-22	-10	OR-21	-8
	Biological Inoculation	OR-12	0	OR-13	0
	Baseline Coring	OR-2	11	OR-2	12
	Oil Release	OR	14	OR	14
	Monitor Coring (BCY1 Only)	OR+3	17		
	Final Coring	OR+13	27	OR+10	24
Extended Experiment	Baseline Coring			ORII-4	24
	Oil Release II			ORII	28
	Final Coring II			ORII+19	47

Appendix Table 3. Oil properties determined for the Alaska North Slope crude oil.

Dynamic Viscosity at 0°C	40	(mPa·s) @ 180s^{-1}
Dynamic Viscosity at 20°C	13	(mPa·s) @ 180s^{-1}
Pour Point	-18	(°C)
Flash Point	< -10	(°C)

Appendix Table 4. Ice thickness at initial and final coring based on extracted core length in Y1 (2014) and Y2 (2015). Acronyms: Oil Release (OR), minus symbol (-) indicates days prior to oil release, plus sign (+) indicates days post oil release.

Year	Day	Tank	Ice Thickness (Mean $\pm$ SD) in cm	Day	Ice Thickness (Mean $\pm$ SD) in cm
1	OR-2	1	17.2 $\pm$ 0.8	OR+13	33.3 $\pm$ 2.4
		2	20.2 $\pm$ 1.1		28.5 $\pm$ 0.8
		3	18.8 $\pm$ 0.5		34.4 $\pm$ 4.8
		4	17.7 $\pm$ 0.8		28.3 $\pm$ 2.7
		5	19.0 $\pm$ 1.1		33.1 $\pm$ 1.5
		6	19.1 $\pm$ 0.9		35.7 $\pm$ 0.7
		All	18.6 $\pm$ 1.35		33.3 $\pm$ 3.7
2	OR-2	1	19.3 $\pm$ 0.3	OR+10	31.1 $\pm$ 0.5
		2	18.4 $\pm$ 3.6		33.6 $\pm$ 1.1
		4	20.0 $\pm$ 1.3		31.3 $\pm$ 1.1
		5	25.2 $\pm$ 2.7		40.2 $\pm$ 1.1
		6	16.0 $\pm$ 1.7		26.6 $\pm$ 3.7
		All	20.2 $\pm$ 3.6		33.0 $\pm$ 4.6

Appendix Table 5. Mean biological parameters of samples taken in Y1 (2014) and Y2 (2015) during biological collections from landfast sea ice in Utqiaġvik, Alaska. Section 0-10 represents the calculated integration of sections spanning 0-10 cm. 0 represents the ice-water interface.

Year	Section (cm)	Chlorophyll a (μg Chl a L^{-1} ice)	EPS (μg XGEQV L^{-1} ice)	Bacterial Abundance (Cells x 10^8 L^{-1} ice)
Y1	0-2	83.0 $+$ 5.2	17,394 $+$ 4,494	14.6 $+$ 3.2
	2-8	20.8 $+$ 6.1	4,883 $+$ 1,142	0.2 $+$ 0.0
	0-10	33.3 $+$ 4.9	7201 $+$ 1,096	3.0 $+$ 0.6
Y2	0-2	246.8 $+$ 10.5	5,388 $+$ 3,504	Not Processed
	2-5	165.9 $+$ 99.5	5,637 $+$ 465	Not Processed
	5-10	28.8 $+$ 2.1	2,540 $+$ 178	Not Processed
	0-10	113.5 $+$ 30.6	3,943 $+$ 601	Not Processed

Appendix Table 6. Mean biological parameters in experiments for full ice cores in Y1 (2014) and Y2 (2015). In Year 2, biota was released below already formed artificial ice; this portion of ice is not included in the full core values. Acronyms: Oil Release (OR), minus symbol (-) indicates days prior to oil release, plus sign (+) indicates days post oil release. Treatments include Biological Control Year 1 (BCY1), Biological Lens Year 1 (BLY1), Oil Lens Year 1 (LY1), Biological Control Year 2 (BCY2), Biological Lens Year 2 (BLY2), Emulsified Oil Year 2 (EOY2). na= not applicable (not collected) *nd*= not detectible (below detection limit)

	Day	Treatment	Chlorophyll a (µg chl a L^{-1}ice)	Algal Abundance (Cells x 10^6 L^{-1} ice)	EPS (µg XGEQV L^{-1} ice)	Bacterial Abundance (Cells x 10^8 L^{-1} ice)
Y1	OR-2	BCY1	2.5 + 0.5	na	556 + 130	3.2 + 1.3
		BLY1	3.5 + 1.4	na	616 + 368	2.6 + 1.8
		LY1	0.0 + 0.0	na	448 + 325	0.3 + 0.6
	OR+3	BCY1	1.5 + 0.4	na	314 + 114	1.3 + 0.7
	OR+13	BCY1	0.7 + 0.3	na	141 + 91	2.2 + 1.2
		BLY1	0.7 + 0.3	na	481 + 330	2.1 + 1.1
		LY1	*nd*	na	292 + 86	0.4 + 0.4
Y2	OR-2	BCY2	3.5 + 0.8	4.1 + 0.7	632 + 30	0.7 + 0.3
		BLY2	2.7 + 0.9	2.6 + 0.9	620 + 36	0.4 + 0.1
		EOY2	4.0 + 2.0	3.3 + 1.3	722 + 158	0.7 + 0.3
	OR+10	BCY2	40.5 + 11.2	25.5 + 1.2	1006 + 211	0.5 + 0.2
		BLY2	5.5 + 5.6	3.4 + 1.4	576 + 195	0.5 + 0.1
		EOY2	5.1 + 5.1	4.2 + 3.2	527 + 86	0.3 + 0.0

Appendix Table 7. Mean biological parameters in experiments for ice sections in Y1 (2014) and Y2 (2015). In Y2, biota was released below already formed artificial ice; this portion of ice is not included in the full core values. Acronyms: Oil Release (OR), (–) indicates days prior to oil release, (+) indicates days post oil release. Treatments include Biological Control Year 1 (BCY1), Biological Lens Year 1 (BLY1), Oil Lens Year 1 (LY1), Biological Control Year 2 (BCY2), Biological Lens Year 2 (BLY2), Emulsified Oil Year 2 (EOY2). 0 cm represents the ice-water interface.

Year	Day	Treatment	Section	Chlorophyll a (μg chl a L^{-1} ice)	Algal Abundance (Cells x 10^6 L^{-1} ice)	EPS (μg XGEQV L^{-1} ice)	Bacterial Abundance (Cells x 10^8 L^{-1} ice)
Y1 (2014)	OR-2	BCY1	0-10.5	3.8 ± 0.8	na	667 ± 231	4.2 ± 2.5
			10.5-19.5	1.3 ± 0.5	na	456 ± 114	2.4 ± 2.3
		BLY1	0-9.5	5.0 ± 1.8	na	951 ± 558	4.2 ± 3.2
			9.5-17.5	2.4 ± 1.3	na	398 ± 134	1.2 ± 0.8
		LY1	0-8	nd	na	686 ± 705	0.0 ± 0.1
			8-18	nd	na	245 ± 99	0.5 ± 1.1
	OR+3	BCY1	0-5	1.2 ± 0.3	na	935 ± 122	2.3 ± 1.4
			5-18.6	1.6 ± 0.5	na	332 ± 166	0.5 ± 0.9
			18.6-28.6	1.8 ± 1.1	na	202 ± 100	1.6 ± 1.7
	OR+13	BCY1	0-5	0.3 ± 0.2	na	394 ± 133	0.7 ± 1.3
			5-26.3	0.6 ± 0.4	na	192 ± 49	1.3 ± 1.1
			26.3-36.3	1.1 ± 0.4	na	223 ± 55	1.7 ± 1.7
		BLY1	0-5	1.0 ± 1.1	na	413 ± 139	1.5 ± 1.5
			5-19	0.8 ± 0.6	na	203 ± 133	0.3 ± 0.5
			19-26.2	0.9 ± 0.4	na	718 ± 718	0.1 ± 0.1
			26.3-33.2	0.3 ± 0.3	na	820 ± 835	8.6 ± 3.9
		LY1	0-5	nd	na	731 ± 327	0.0 ± 0.0
			5-18.2	nd	na	94 ± 142	0.0 ± 0.0
			17.5-24.3	nd	na	325 ± 96	0.0 ± 0.1
			24.3-30.6	nd	na	363 ± 231	2.0 ± 1.4
Y2 (2015)	OR-2	BCY2	9.1-13.3	4.3 ± 0.8	6.5 ± 1.8	744 ± 82	0.8 ± 0.4
			13.3-18.3	2.7 ± 2.0	4.8 ± 1.8	542 ± 71	0.9 ± 0.5
		BLY2	13.4-17.6	3.0 ± 1.2	2.6 ± 0.6	601 ± 39	0.4 ± 0.2
			17.6-22.6	2.4 ± 0.6	1.8 ± 0.6	638 ± 16	0.5 ± 0.3
		EOY2	9.8-14.3	4.4 ± 0.7	4.7 ± 1.8	764 ± 80	1.0 ± 0.5
			12.7-17.7	3.9 ± 1.8	2.5 ± 1.0	715 ± 113	0.4 ± 0.1
	OR+10	BCY2	16.6-20.9	3.0 ± 1.5	3.7 ± 2.9	885 ± 241	0.6 ± 0.2
			20.9-25.9	10.6 ± 5.9	12.3 ± 14.1	761 ± 49	0.6 ± 0.2
			25.9-33.6	79.9 ± 26.0	31.1 ± 31.2	$1,257 \pm 520$	0.9 ± 0.4
		BLY2	16.3-21.3	1.5 ± 1.3	1.2 ± 0.1	463 ± 33	0.2 ± 0.2
			21.3-26.3	2.6 ± 0.4	3.1 ± 1.2	506 ± 35	0.3 ± 0.1
			26.3-35.75	8.3 ± 7.2	5.6 ± 3.7	577 ± 96	0.2 ± 0.1
		EOY2	18-22.6	1.2 ± 0.7	6.5 ± 2.1	549 ± 46	0.6 ± 0.3
			19.3-24.3	2.4 ± 0.9	3.8 ± 1.6	568 ± 135	0.3 ± 0.0
			24.3-28.9	10.2 ± 4.6	13.6 ± 11.6	655 ± 205	0.5 ± 0.2

Appendix Table 8. Individual section measurements for biological cores.

year	sample day	tank	treatment	replication	section depth top (cm)	section depth bottom (cm)	section length (cm)	total length (cm)	µg Chl a l^{-1}	EPS µg XGEQV l^{-1}	bacteria (x10^8 l^{-1})	diatoms (x10^6 l^{-1})	diatoms w/ plastids (x10^6 l^{-1})	diatoms w/o plastids (x10^6 l^{-1})	frustules (x10^6 l^{-1})
2014	ENV	ENV	ENV	A	124	132	8	134	23.5	5757.0	0.2				
2014	ENV	ENV	ENV	A	132	134	2	134	77.4	12938.0	11.0				
2014	ENV	ENV	ENV	B	127	135	8	137	25.2	4969.5	0.2				
2014	ENV	ENV	ENV	B	135	137	2	137	87.5	21628.4	15.5				
2014	ENV	ENV	ENV	C	125	133	8	135	13.9	3558.6	0.2				
2014	ENV	ENV	ENV	C	133	135	2	135	84.1	16312.9	17.1				
2014	OR-2	1	BLY1	A	0	6.5	6.5	16.5	4.5	535.8	0.1				
2014	OR-2	1	BLY1	A	6.5	10.5	4	16.5	0.2		0.1				
2014	OR-2	1	BLY1	A	10.5	14.5	4	16.5	0.9		0.1				
2014	OR-2	1	BLY1	A	14.5	15.5	1	16.5	0.4		0.1				
2014	OR-2	1	BLY1	A	15.5	16.5	1	16.5	0.1		0.1				
2014	OR-2	1	BLY1	B	0	7.7	7.7	17.7	2.5	787.3	2.5				
2014	OR-2	1	BLY1	B	7.7	17.7	10	17.7	1.9	451.2	2.5				
2014	OR-2	1	BLY1	C	0	8.3	8.3	18.3	5.5	1403.3	2.9				
2014	OR-2	1	BLY1	C	8.3	18.3	10	18.3	1.4	540.6	1.4				
2014	OR-2	2	BCY1	A	0	11.4	11.4	21.4	4.4	465.1	2.9				
2014	OR-2	2	BCY1	A	11.4	20.4	9	21.4	0.7	149.6	7.6				
2014	OR-2	2	BCY1	A	20.4	21.4	1	21.4	0.3	1625.7	0.1				
2014	OR-2	2	BCY1	B	0	9.4	9.4	19.4	4.4	925.0	7.4				
2014	OR-2	2	BCY1	B	9.4	19.4	10	19.4	2.0	589.2	0.2				
2014	OR-2	2	BCY1	C	0	9.3	9.3	19.3	3.9	332.8	0.5				
2014	OR-2	2	BCY1	C	9.3	19.3	10	19.3	1.5	531.1	1.7				
2014	OR-2	3	LY1	A	0.3	8.3	8	18.3	0.0	371.4	0.2				
2014	OR-2	3	LY1	A	8.3	18.3	10	18.3	0.0	410.6	0.0				
2014	OR-2	3	LY1	B	0	9.5	9.5	19.5	0.0	475.9	0.0				
2014	OR-2	3	LY1	B	9.5	19.5	10	19.5	0.0	308.0	0.3				
2014	OR-2	3	LY1	C	0	8.7	8.7	18.7	0.0	2120.8	0.0				
2014	OR-2	3	LY1	C	8.7	18.7	10	18.7	0.0	209.3	0.0				
2014	OR-2	4	LY1	A	0	8.3	8.3	18.3	0.0	320.6	0.0				
2014	OR-2	4	LY1	A	8.3	18.3	10	18.3	0.0	172.2	0.0				
2014	OR-2	4	LY1	B	0	8.2	8.2	18.2	0.0	397.2	0.0				

year	sample day	tank	treatment	replication	section depth top (cm)	section depth bottom (cm)	section length (cm)	total length (cm)	µg Chl a l^{-1}	EPS µg XGEQV l^{-1}	bacteria (x10^8 l^{-1})	diatoms (x10^6 l^{-1})	diatoms w/ plastids (x10^6 l^{-1})	diatoms w/o plastids (x10^6 l^{-1})	frustules (x10^6 l^{-1})
2014	OR-2	4	LY1	B	8.2	18.2	10	18.2	0.0	141.1	2.7				
2014	OR-2	4	LY1	C	0	6.7	6.7	16.7	0.0	427.3	0.0				
2014	OR-2	4	LY1	C	6.7	16.7	10	16.7	0.0	228.8	0.0				
2014	OR-2	5	BLY1	A	0	7.7	7.7	17.7	7.8	735.1	4.8				
2014	OR-2	5	BLY1	A	7.7	17.7	10	17.7	4.1	270.1	0.4				
2014	OR-2	5	BLY1	B	0	10	10	20	4.0	1846.3	5.0				
2014	OR-2	5	BLY1	B	10	20	10	20	3.3	485.4	1.5				
2014	OR-2	5	BLY1	C	0	9.4	9.4	19.4	5.4	399.2	9.6				
2014	OR-2	5	BLY1	C	9.4	19.4	10	19.4	3.1	241.5	1.7				
2014	OR-2	6	BCY1	A	0	10.2	10.2	20.2	2.4	634.9	5.0				
2014	OR-2	6	BCY1	A	10.2	20.2	10	20.2	1.0	539.6	2.0				
2014	OR-2	6	BCY1	B	0	8.3	8.3	18.3	4.3	832.7	3.2				
2014	OR-2	6	BCY1	B	8.3	18.3	10	18.3	0.8	406.4	1.8				
2014	OR-2	6	BCY1	C	0	8.7	8.7	18.7	3.6	808.8	6.0				
2014	OR-2	6	BCY1	C	8.7	18.7	10	18.7	1.7	374.3	1.8				
2014	OR+3	2	BCY1	A	0	5	5	29.5	1.0	802.3	1.5				
2014	OR+3	2	BCY1	A	5	19.5	14.5	29.5	2.5		0.2				
2014	OR+3	2	BCY1	A	19.5	29.5	10	29.5		152.6	1.3				
2014	OR+3	2	BCY1	B	0	5	5	28	1.1	913.4	0.1				
2014	OR+3	2	BCY1	B	5	18	13	28	2.0	139.9	0.3				
2014	OR+3	2	BCY1	B	18	28	10	28	2.5	91.9	1.6				
2014	OR+3	2	BCY1	C	0	5	5	27.9	0.7	926.0	1.9				
2014	OR+3	2	BCY1	C	5	17.9	12.9	27.9	1.2		0.1				
2014	OR+3	2	BCY1	C	17.9	27.9	10	27.9	0.8	129.5	1.8				
2014	OR+3	6	BCY1	A	0	5	5	27.9	1.4	1105.6	3.1				
2014	OR+3	6	BCY1	A	5	17.9	12.9	27.9	1.3		2.3				
2014	OR+3	6	BCY1	A	17.9	27.9	10	27.9	2.5	367.1	0.2				
2014	OR+3	6	BCY1	B	0	5	5	27.8	1.5	812.6	3.3				
2014	OR+3	6	BCY1	B	5	17.8	12.8	27.8	1.5	436.2	0.1				

year	sample day	tank	treatment	replication	section depth top (cm)	section depth bottom (cm)	section length (cm)	total length (cm)	µg Chl a l⁻¹	EPS µg XGEQV l⁻¹	bacteria (x10⁸ l⁻¹)	diatoms (x10⁶ l⁻¹)	diatoms w/ plastids (x10⁶ l⁻¹)	diatoms w/o plastids (x10⁶ l⁻¹)	frustules (x10⁶ l⁻¹)
2014	OR+3	6	BCY1	B	17.8	27.8	10	27.8	2.5	210.6	4.9				
2014	OR+3	6	BCY1	C	0	5	5	30.5	1.6	1047.7	3.7				
2014	OR+3	6	BCY1	C	5	20.5	15.5	30.5	1.3	418.6	0.1				
2014	OR+3	6	BCY1	C	20.5	30.5	10	30.5	0.4	257.6	0.1				
2014	OR+13	1	BLY1	A	0	5	5	36.5	0.6	289.4	0.1				
2014	OR+13	1	BLY1	A	5	19.5	14.5	36.5	1.8	348.7	0.2				
2014	OR+13	1	BLY1	A	19.5	26.5	7	36.5	1.1	425.4	0.1				
2014	OR+13	1	BLY1	A	26.5	36.5	10	36.5	0.7	401.3	6.6				
2014	OR+13	1	BLY1	B	0	5	5	32.5	0.8	381.5	3.5				
2014	OR+13	1	BLY1	B	5	19.5	14.5	32.5	0.7	0.9	0.1				
2014	OR+13	1	BLY1	B	19.5	24.5	5	32.5	1.3	299.4	0.2				
2014	OR+13	1	BLY1	B	24.5	32.5	8	32.5	0.1	432.2	4.2				
2014	OR+13	1	BLY1	C	0	5	5	31	3.2	475.6	0.4				
2014	OR+13	1	BLY1	C	5	16.5	11.5	31	0.8	267.9	0.2				
2014	OR+13	1	BLY1	C	16.5	23	6.5	31	0.6	285.7	0.2				
2014	OR+13	1	BLY1	C	23	31	8	31	0.1	389.0	15.0				
2014	OR+13	2	BCY1	A	0	5	5	37	0.2	502.8	0.1				
2014	OR+13	2	BCY1	A	5	27	22	37	0.8	252.9	1.4				
2014	OR+13	2	BCY1	A	27	37	10	37	0.9	184.4	0.3				
2014	OR+13	2	BCY1	B	0	5	5	37.8	0.4	521.9	0.2				
2014	OR+13	2	BCY1	B	5	27.8	22.8	37.8	0.0	156.0	0.2				
2014	OR+13	2	BCY1	B	27.8	37.8	10	37.8	1.0		2.8				
2014	OR+13	2	BCY1	C	0	5	5	35.9	0.2	433.3	0.0				
2014	OR+13	2	BCY1	C	5	25.9	20.9	35.9	0.8	148.5	1.8				
2014	OR+13	2	BCY1	C	25.9	35.9	10	35.9	1.5		3.8				
2014	OR+13	3	LY1	A	0	5	5	39.5	0.0	663.7	0.0				
2014	OR+13	3	LY1	A	5	18.5	13.5	39.5	-0.1	95.5	0.0				
2014	OR+13	3	LY1	A	18.5	27.5	9	39.5	-0.1	90.0	0.0				
2014	OR+13	3	LY1	A	27.5	39.5	12	39.5	0.0	297.7	3.2				

year	sample day	tank	treatment	replication	section depth top (cm)	section depth bottom (cm)	section length (cm)	total length (cm)	µg Chl a l^{-1}	EPS µg XGEQV l^{-1}	bacteria (x10^8 l^{-1})	diatoms (x10^6 l^{-1})	diatoms w/ plastids (x10^6 l^{-1})	diatoms w/o plastids (x10^6 l^{-1})	frustules (x10^6 l^{-1})
2014	OR+13	3	LY1	B	0	4.2	4.2	28	0.0	1055.7	0.0				
2014	OR+13	3	LY1	B	4.2	19	14.8	28	0.0	98.2	0.0				
2014	OR+13	3	LY1	B	19	28	9	28	-0.6	165.1	0.1				
2014	OR+13	3	LY1	C	0	5	5	34	-0.4	751.4	0.0				
2014	OR+13	3	LY1	C	5	19	14	34	-0.2	366.1	0.0				
2014	OR+13	3	LY1	C	14.8	22.8	8	34	-0.7	121.5	0.2				
2014	OR+13	3	LY1	C	27	34	7	34	-0.1	405.7	3.4				
2014	OR+13	4	LY1	A	0	5	5	28.3	-0.2	780.3	0.0				
2014	OR+13	4	LY1	A	5	18.8	13.8	28.3	-0.1	0.9	0.0				
2014	OR+13	4	LY1	A	18.8	23.3	4.5	28.3	-0.8	1042.3	0.0				
2014	OR+13	4	LY1	A	23.3	28.3	5	28.3	-0.2	0.9	1.5				
2014	OR+13	4	LY1	B	0	5	5	25.1	-0.1	139.7	0.0				
2014	OR+13	4	LY1	B	5	16.6	11.6	25.1	-0.1	0.9	0.0				
2014	OR+13	4	LY1	B	16.6	21.4	4.8	25.1	-0.3	323.7	0.0				
2014	OR+13	4	LY1	B	21.4	25.1	3.7	25.1	-0.2	599.0	0.0				
2014	OR+13	4	LY1	C	0	5	5	31.4	0.0	997.3	0.0				
2014	OR+13	4	LY1	C	5	17.4	12.4	31.4	-0.1	0.9	0.0				
2014	OR+13	4	LY1	C	17.4	25.4	8	31.4	-0.1	573.6	0.0				
2014	OR+13	4	LY1	C	25.4	31.4	6	31.4	0.0	509.0	2.1				
2014	OR+13	5	BLY1	A	0	5	5	34.5	0.7	354.7	3.4				
2014	OR+13	5	BLY1	A	5	19	14	34.5	0.7	92.3	1.3				
2014	OR+13	5	BLY1	A	19	26.5	7.5	34.5	1.1	2125.9	0.1				
2014	OR+13	5	BLY1	A	26.5	34.5	8	34.5	0.3	2511.4	6.9				
2014	OR+13	5	BLY1	B	0	5	5	31.1	0.8	663.7	1.1				
2014	OR+13	5	BLY1	B	5	18.5	13.5	31.1	0.0	204.9	0.1				
2014	OR+13	5	BLY1	B	18.5	27.5	9	31.1	0.3	351.7	0.0				
2014	OR+13	5	BLY1	B	27.5	31.1	3.6	31.1	0.6	671.3	7.5				
2014	OR+13	5	BLY1	C	0	5	5	33.7	0.2	314.4	0.4				
2014	OR+13	5	BLY1	C	5	21	16	33.7	0.7	302.7	0.1				

year	sample day	tank	treatment	replication	section depth top (cm)	section depth bottom (cm)	section length (cm)	total length (cm)	µg Chl a l^{-1}	EPS µg XGEQV l^{-1}	bacteria (x10^8 l^{-1})	diatoms (x10^6 l^{-1})	diatoms w/ plastids (x10^6 l^{-1})	diatoms w/o plastids (x10^6 l^{-1})	frustules (x10^6 l^{-1})
2014	OR+13	5	BLY1	C	21	29.7	8.7	33.7	0.7	816.7	0.1				
2014	OR+13	5	BLY1	C	29.7	33.7	4	33.7	0.2	515.9	11.2				
2014	OR+13	6	BCY1	A	0.3	5.3	5	35.5	0.5		0.1				
2014	OR+13	6	BCY1	A	5.3	25.5	20.2	35.5	1.0	211.5	3.2				
2014	OR+13	6	BCY1	A	25.5	35.5	10	35.5	1.6	261.5	8.2				
2014	OR+13	6	BCY1	B	0	5	5	36.5	0.1	291.2	0.3				
2014	OR+13	6	BCY1	B	5	26.5	21.5	36.5	0.1		1.1				
2014	OR+13	6	BCY1	B	26.5	36.5	10	36.5	1.1		7.1				
2014	OR+13	6	BCY1	C	0	5	5	35	0.2	219.9	3.2				
2014	OR+13	6	BCY1	C	5	25	20	35	0.9		0.2				
2014	OR+13	6	BCY1	C	25	35	10	35	0.7		6.9				
2015	ENV	ENV	ENV	A	117	122	5	127	26.8	2290.8					
2015	ENV	ENV	ENV	A	122	125	3	127	52.2	5950.5					
2015	ENV	ENV	ENV	A	125	127	2	127	245.9	2389.5					
2015	ENV	ENV	ENV	B	117	122	5	127	30.9	2547.1					
2015	ENV	ENV	ENV	B	122	125	3	127	208.7	5042.9					
2015	ENV	ENV	ENV	B	125	127	2	127	257.9	9034.5					
2015	ENV	ENV	ENV	C	117	122	5	127	28.7	2622.7					
2015	ENV	ENV	ENV	C	122	125	3	127	236.7	5496.7					
2015	ENV	ENV	ENV	C	125	127	2	127	236.7	4337.0					
2015	OR-2	1	EOY2	A	10	14.5	4.5	19.5	4.2	854.0	0.6	5.0	5.0	0.0	0.2
2015	OR-2	1	EOY2	A	14.5	19.5	5	19.5	4.2	686.3	0.6	3.7	3.7	0.0	0.0
2015	OR-2	1	EOY2	B	9.5	14.5	5	19.5	3.7	734.8	0.4	4.1	4.1	0.0	0.0
2015	OR-2	1	EOY2	B	14.5	19.5	5	19.5	4.0	698.2	0.4	3.7	3.6	0.1	0.2
2015	OR-2	1	EOY2	C	10	14	4	19	5.1	702.8	1.5	6.6	6.6	0.0	0.0
2015	OR-2	1	EOY2	C	14	19	5	19	3.1	821.5	0.9	2.9	2.9	0.0	0.0
2015	OR-2	2	BCY2	A	6.5	10.5	4	15.5	5.0	834.7	0.6	7.2	6.9	0.3	0.2
2015	OR-2	2	BCY2	A	10.5	15.5	5	15.5	3.1	503.5	0.5	3.1	3.1	0.0	0.0
2015	OR-2	2	BCY2	B	6.8	11.8	5	16.8	4.6	675.0	1.4	2.9	2.7	0.2	0.0

year	sample day	tank	treatment	replication	section depth top (cm)	section depth bottom (cm)	section length (cm)	total length (cm)	µg Chl a l⁻¹	EPS µg XGEQV l⁻¹	bacteria (x10⁸ l⁻¹)	diatoms (x10⁶ l⁻¹)	diatoms w/ plastids (x10⁶ l⁻¹)	diatoms w/o plastids (x10⁶ l⁻¹)	frustules (x10⁶ l⁻¹)
2015	OR-2	2	BCY2	B	11.8	16.8	5	16.8	0.6	623.3	0.7	4.4	4.4	0.0	0.3
2015	OR-2	2	BCY2	C	14	18	4	23	3.5	720.9	0.6	5.0	4.8	0.2	0.0
2015	OR-2	2	BCY2	C	18	23	5	23	4.5	498.3	0.2	2.5	2.4	0.1	0.0
2015	OR-2	4	BLY2	A	8.5	13.5	5	18.5	1.7	691.2	0.7	2.8	2.8	0.0	0.0
2015	OR-2	4	BLY2	A	13.5	18.5	5	18.5	3.1	607.6	0.5	2.3	2.3	0.0	0.0
2015	OR-2	4	BLY2	B	10	15	5	20	5.2	596.7	0.5	2.6	2.6	0.0	0.1
2015	OR-2	4	BLY2	B	15	20	5	20	2.7	695.8	0.5	2.0	2.0	0.0	0.0
2015	OR-2	4	BLY2	C	16.4	21.4	5	21.4	1.9	585.7	0.9	3.7	3.5	0.2	0.0
2015	OR-2	4	BLY2	C	16.4	21.4	5	21.4	4.2	714.8	0.4	4.6	4.5	0.2	0.2
2015	OR-2	5	BLY2	A	12	17	5	22	2.7	580.2	0.3	3.4	3.4	0.1	0.0
2015	OR-2	5	BLY2	A	17	22	5	22	2.8	632.7	0.3	2.4	2.4	0.0	0.0
2015	OR-2	5	BLY2	B	15.5	20.5	5	25.5	3.6	619.3	0.4	2.8	2.8	0.0	0.0
2015	OR-2	5	BLY2	B	20.5	25.5	5	25.5	2.4	594.9	0.3	1.4	1.4	0.0	0.0
2015	OR-2	5	BLY2	C	18	23	5	28	0.9	403.2	0.2	1.7	1.7	0.0	0.0
2015	OR-2	5	BLY2	C	23	28	5	28	1.8	713.6	0.4	1.0	1.0	0.0	0.0
2015	OR-2	6	EOY2	A	10	15	5	15	4.0	968.9	0.8	2.9	2.9	0.0	0.1
2015	OR-2	6	EOY2	B	10	15	5	15	7.2	503.9	0.6	3.4	3.4	0.0	0.0
2015	OR-2	6	EOY2	C	13	18	5	18	1.0	608.8	0.4	0.9	0.9	0.0	0.0
2015	OR+10	1	EOY2	A	16	20.5	4.5	30.5	0.4	599.9	0.6	1.7	1.0	0.7	1.4
2015	OR+10	1	EOY2	A	20.5	25.5	5	30.5	0.9	479.6	0.2	3.6	2.0	1.5	1.2
2015	OR+10	1	EOY2	A	25.5	30.5	5	30.5	0.7	440.6	0.5	0.1	0.0	0.1	0.3
2015	OR+10	1	EOY2	B	18.2	22.7	4.5	31.7	1.6	509.4	0.3	4.2	3.1	1.1	0.6
2015	OR+10	1	EOY2	B	22.7	27.7	5	31.7	4.4	681.9	0.2	4.2	0.4	3.8	0.2
2015	OR+10	1	EOY2	B	27.7	31.7	4	31.7	2.8	491.9	0.3	1.7	0.3	1.4	0.4
2015	OR+10	1	EOY2	C	20	24.5	4.5	31.2	1.7	537.7	0.4	2.7	2.0	0.7	1.8
2015	OR+10	1	EOY2	C	24.5	29.5	5	31.2	1.0	371.0	0.3	4.3	0.1	4.3	0.6
2015	OR+10	1	EOY2	C	29.5	31.2	1.7	31.2	0.9		0.4	0.3	0.0	0.3	0.4
2015	OR+10	2	BCY2	A	17.7	21.7	4	32.7	4.1	926.9	0.3	7.0	6.0	1.0	2.3
2015	OR+10	2	BCY2	A	21.7	26.7	5	32.7	17.2	806.0	0.7	28.5	28.1	0.4	0.4

year	sample day	tank	treatment	replication	section depth top (cm)	section depth bottom (cm)	section length (cm)	total length (cm)	µg Chl a l^{-1}	EPS µg XGEQV l^{-1}	bacteria (x10^8 l^{-1})	diatoms (x10^6 l^{-1})	diatoms w/ plastids (x10^6 l^{-1})	diatoms w/o plastids (x10^6 l^{-1})	frustules (x10^6 l^{-1})
2015	OR+10	2	BCY2	A	26.7	32.7	6	32.7	71.9	1819.1	1.0	67.1	66.2	0.9	0.3
2015	OR+10	2	BCY2	B	15	19	4	33	3.5	626.5	0.7	8.5	7.8	0.7	3.2
2015	OR+10	2	BCY2	B	19	24	5	33	8.8	767.4	0.4	11.0	10.6	0.4	0.2
2015	OR+10	2	BCY2	B	24	33	9	33	58.8	1162.2	0.6	39.0	38.6	0.4	0.0
2015	OR+10	2	BCY2	C	18	22	4	35	1.3	1102.3	0.2	3.1	2.8	0.3	0.2
2015	OR+10	2	BCY2	C	22	27	5	35	5.8	709.8	0.3	8.6	8.5	0.1	0.4
2015	OR+10	2	BCY2	C	27	35	8	35	108.9	791.5	0.4	22.7	22.4	0.3	0.0
2015	OR+10	3	BCY2	B	22.5	27.5	5	27.5	133.0	3262.5					
2015	OR+10	4	BLY2	A	12.4	17.4	5	32.4	0.4	528.6	0.4	1.2	0.0	1.2	0.9
2015	OR+10	4	BLY2	A	17.4	22.4	5	32.4	0.5	540.1	0.3	0.7	0.1	0.6	1.1
2015	OR+10	4	BLY2	A	22.4	32.4	10	32.4	5.0	284.5	0.2	2.4	0.0	2.4	0.8
2015	OR+10	4	BLY2	B	12.1	17.1	5	31.6	4.0	402.8	0.4	4.6	0.6	4.0	0.4
2015	OR+10	4	BLY2	B	17.1	22.1	5	31.6	2.8	470.3	0.3	3.4	0.1	3.3	0.9
2015	OR+10	4	BLY2	B	22.1	31.6	9.5	31.6	4.6	413.5	0.3	2.3	1.2	1.2	0.0
2015	OR+10	4	BLY2	C	13	18	5	30	0.6	464.7	0.4	1.2	0.0	1.2	1.0
2015	OR+10	4	BLY2	C	18	23	5	30	2.0	529.0	0.4	2.3	0.0	2.3	0.9
2015	OR+10	4	BLY2	C	23	30	7	30	11.5	640.7	0.2	2.0	0.0	2.0	1.4
2015	OR+10	5	BLY2	A	20	25	5	40	1.4	472.9	0.2	0.5	0.3	0.2	0.5
2015	OR+10	5	BLY2	A	25	30	5	40	3.7	551.2	0.3	2.1	1.9	0.2	0.0
2015	OR+10	5	BLY2	A	30	40	10	40	0.6	697.0	0.2	6.4	0.0	6.4	0.0
2015	OR+10	5	BLY2	B	21.5	26.5	5	41.5	2.0	471.5	0.5	2.5	2.2	0.3	0.2
2015	OR+10	5	BLY2	B	26.5	31.5	5	41.5	3.1	494.9	0.2	1.5	1.4	0.1	0.2
2015	OR+10	5	BLY2	B	31.5	41.5	10	41.5	27.7	697.0	0.2	7.0	6.8	0.3	0.1
2015	OR+10	5	BLY2	C	19	24	5	39	0.7	438.3	0.3	1.0	0.1	0.8	1.0
2015	OR+10	5	BLY2	C	24	29	5	39	3.4	448.3	0.3	1.5	1.2	0.3	0.3
2015	OR+10	5	BLY2	C	29	39	10	39	1.5	707.9	0.3	8.9	0.1	8.8	0.2
2015	OR+10	6	EOY2	A	12	17	5	26	4.4	865.8	0.2	2.0	1.4	0.6	0.2
2015	OR+10	6	EOY2	A	17	26	9	26	21.7	999.9	1.0	15.1	4.7	10.4	1.0
2015	OR+10	6	EOY2	B	23	28	5	31	2.0	550.5	0.4	2.6	1.8	0.8	0.7

year	sample day	tank	treatment	replication	section depth top (cm)	section depth bottom (cm)	section length (cm)	total length (cm)	µg Chl a l^{-1}	EPS µg XGEQV l^{-1}	bacteria (x10^8 l^{-1})	diatoms (x10^6 l^{-1})	diatoms w/ plastids (x10^6 l^{-1})	diatoms w/o plastids (x10^6 l^{-1})	frustules (x10^6 l^{-1})
2015	OR+10	6	EOY2	B	28	31	3	31	8.4	535.2	0.6	2.1	1.1	1.0	4.2
2015	OR+10	6	EOY2	C	12.9	17.9	5	22.9	2.0	460.1	0.3	1.8	1.6	0.3	0.7
2015	OR+10	6	EOY2	C	17.9	22.9	5	22.9	14.8	548.6	0.7	6.2	3.8	2.4	0.0
2015	ORII	2	Emulsified II	A	27.3	32.3	5	45	7.7	1203.0					
2015	ORII	2	Emulsified II	A	32.3	38.3	6	45	35.3	1814.3					
2015	ORII	2	Emulsified II	A	38.3	43.3	5	45	155.1	3493.0					
2015	ORII	2	Emulsified II	A	43.3	45	1.7	45	357.6	10633.7					
2015	ORII	3	Emulsified II	A	20	23	3	30.5	256.6	4831.6					
2015	ORII	3	Emulsified II	A	23	26.5	3.5	30.5	0.0	5044.5					
2015	ORII	3	Emulsified II	A	26.5	30.5	4	30.5	145.5	3320.4					
2015	ORII+19	2	Emulsified II	A	14.5	23.5	9	42.5	582.5	3567.0					
2015	ORII+19	2	Emulsified II	A	23.5	28.5	5	42.5	3.0	906.1					
2015	ORII+19	2	Emulsified II	A	28.5	33.5	5	42.5	17.0	1345.4					
2015	ORII+19	2	Emulsified II	A	33.5	42.5	9	42.5	57.2	1790.4					
2015	ORII+19	2	Emulsified II	B	15.7	24.7	9	43.7	17.9	3784.1					
2015	ORII+19	2	Emulsified II	B	24.7	29.7	5	43.7	0.7	1780.7					
2015	ORII+19	2	Emulsified II	B	29.7	34.7	5	43.7	9.0	1031.1					
2015	ORII+19	2	Emulsified II	B	34.7	43.7	9	43.7	40.0	3003.7					
2015	ORII+19	2	Emulsified II	C	17.5	26.5	9	47.5	181.0	2980.2					
2015	ORII+19	2	Emulsified II	C	26.5	31.5	5	47.5	1.5	822.9					
2015	ORII+19	2	Emulsified II	C	31.5	36.5	5	47.5	1.6	929.5					
2015	ORII+19	2	Emulsified II	C	36.5	47.5	11	47.5	19.1	793.9					
2015	ORII+19	3	Emulsified II	A	37.5	42.5	5	49	19.9	3482.1					
2015	ORII+19	3	Emulsified II	A	42.5	49	6.5	49	55.5	1228.6					
2015	ORII+19	3	Emulsified II	B	39	44	5	49	397.2	3371.2					
2015	ORII+19	3	Emulsified II	B	44	49	5	49	43.7	1258.4					
2015	ORII+19	3	Emulsified II	C	39.5	44.5	5	49.5	13.2	2759.8					
2015	ORII+19	3	Emulsified II	C	44.5	49.5	5	49.5	57.0	1706.4					

Appendix Table 9. Physical data collected from field sampling in Utqiaġvik, Alaska.

Year	Depth Mid-Point (m)	Temperature	Bulk Salinity	Brine Salinity	Brine Volume Fraction (%)
2014	0.000	-14.3			
2014	0.025	-14	8.7	172.3	3.7
2014	0.075	-12.5	7.4	162.3	3.4
2014	0.125	-11.8	6.2	157.2	3.0
2014	0.175	-11.2	5.2	152.7	2.6
2014	0.225	-9.7	5.2	140.2	2.9
2014	0.275	-10.3	5.5	145.4	2.9
2014	0.325	-10.6	5.7	147.9	3.0
2014	0.375	-9.5	5.9	138.4	3.3
2014	0.425	-9.3	5.8	136.5	3.4
2014	0.475	-8.6	5.9	129.9	3.6
2014	0.525	-6.8	5.5	110.3	4.1
2014	0.575	-7.5	5.6	118.0	3.9
2014	0.625	-7.4	5.3	117.1	3.7
2014	0.675	-6.7	5.1	109.1	3.9
2014	0.725	-6.0	4.8	100.5	4.0
2014	0.775	-6.1	4.5	101.1	3.7
2014	0.825	-5.3	4.9	91.2	4.6
2014	0.875	-5.2	4.9	90.2	4.7
2014	0.925	-5.0	5.5	87.0	5.4
2014	0.975	-4.5	4.8	79.7	5.2
2014	1.025	-4.1	4.6	72.8	5.5
2014	1.075	-3.8	4.6	68.7	5.8
2014	1.125	-3.6	5.8	65.7	7.7
2014	1.175	-3.0	5.4	54.8	8.8
2014	1.225	-2.0	5.6	37.6	13.5
2014	1.275	-2.4	6.7	45.4	13.2
2014	1.325	-2.0	6.5	37.6	15.8
2014	1.340	-1.8	8.8	32.8	24.6
2015	0	-16.9			
2015	0.025	-15.7	9.1	182.8	3.6
2015	0.075	-15.8	8.3	183.4	3.3
2015	0.125	-15.6	6.9	182.2	2.7
2015	0.175	-13.7	6.9	170.3	3.0
2015	0.22		6.3	172.3	2.7
2015	0.225	-14			
2015	0.27		6.9	175.4	2.9
2015	0.275	-14.5			
2015	0.325	-14	6.8	172.3	2.9
2015	0.375	-12.5	6.1	162.3	2.8
2015	0.425	-12.4			
2015	0.43		5.5	161.5	2.6

Year	Depth Mid-Point (m)	Temperature	Bulk Salinity	Brine Salinity	Brine Volume Fraction (%)
2015	0.48		5.2		
2015	0.525		5.5		
2015	0.575		5.8		
2015	0.625	-10	5.4	142.8	3.0
2015	0.675	-9.5	5.9	138.4	3.4
2015	0.725	-8.8	5.4	131.8	3.3
2015	0.775	-7.8	5.5	121.6	3.7
2015	0.825	-7.6	5.6	119.4	3.8
2015	0.875	-7.2	5.3	115.0	3.8
2015	0.92		5.3	105.5	4.2
2015	0.925	-6.4			
2015	0.97		6.1	107.9	4.7
2015	0.975	-6.6			
2015	1.025	-5.4	5.5	92.5	5.0
2015	1.075	-4.5	5.5	79.7	6.0
2015	1.125	-3.8	5.1	68.9	6.4
2015	1.175	-3.2	6.6	59.0	9.9
2015	1.225	-2.5	6.9	46.8	13.2
2015	1.26		9.1	40.4	20.9

Appendix Table 10. Tank monitoring data from Y2 (2015).

Date	Time	Tank	Surface Temperature (˚C)	Water Temperature (˚C)	Water Salinity	Ice Thickness (cm)	2π Surface Irradiance (μmol photons m^{-2} s^{-1})
3/24/2015	17:45	1		-1.6		9	
3/25/2015	12:00	1		-1.3	29.3	13	
3/26/2015	9:00	1	-7.7	-1.3	30	13	
3/28/2015	11:21	1	-7.6	-1.4	30.4		243.4
3/29/2015	14:31	1	-7.2	-1.4	30.7		244.2
3/30/2015	11:30	1	-7.7	-1.3	30.7		244.4
3/31/2015	19:31	1	-10	-1.4	31.2		246.2
4/1/2015	17:00	1	-8.7	-1.4	31.3		244
4/2/2015	11:43	1	-8.8	-1.4	31.4		246.3
4/3/2015	16:30	1	-9.9	-1.3	31.6		242.5
4/4/2015	12:30	1	-8.6	-1.3	31.5		242.8
4/5/2015	14:00	1	-8.5	-1.3	32		242.9
4/6/2015	9:30	1	-8.8	-1.3	32.1		248.2
4/8/2015	11:00	1	-9.8	-1.4	32.7		289.5
4/10/2015	18:00	1	-9.9	-1.4	22.5		299.8
4/12/2015	13:52	1	-11.7	-1.5			305.7
4/13/2015	9:21	1	-11.6	-1.6			307.2
4/14/2015	3:00	1	-11.8	-1.7			305.2
4/16/2015	13:00	1	-10	-1.8			301.5
3/24/2015	17:45	2				9	
3/25/2015	12:00	2		-1.68		12	
3/26/2015	9:00	2	-7.6	-1.6		12.5	
3/28/2015	11:21	2	-6.3		31.7		231.9
3/29/2015	14:31	2	-7.2		31.3		231.5
3/30/2015	11:30	2	-7.6		31.3		234
3/31/2015	19:31	2	-7.5		32.2		237.6
4/1/2015	17:00	2	-9.5		32.3		233.8
4/2/2015	11:43	2	-9.3		32.7		238
4/3/2015	16:30	2	-9.3		31.7		239
4/4/2015	12:30	2	-8.9		33.1		230.2
4/5/2015	14:00	2	-8.7		33.1		235.2
4/6/2015	9:30	2	-8.5		33.3		238.2
4/8/2015	11:00	2	-10.2		33.7		295.1
4/10/2015	18:00	2	-8.6		34.9		303.2
4/12/2015	13:52	2	-9.4		34.7		283.1
4/13/2015	9:21	2	-9.3		34.7		285.2
4/14/2015	3:00	2	-9.5		35.1		286.1
4/16/2015	13:00	2	-10.3		34.3		285.3
3/24/2015	17:45	3		-1.6	28	9	
3/25/2015	12:00	3		-1.6	29.2	12	

Date	Time	Tank	Surface Temperature (˚C)	Water Temperature (˚C)	Water Salinity	Ice Thickness (cm)	2π Surface Irradiance (μmol photons m^{-2} s^{-1})
3/26/2015	9:00	3	-6.7	-1.6	30.4	14	
3/28/2015	11:21	3	-7.4	-1.7	30.9	15	239.9
3/29/2015	14:31	3	-7.6	-1.7	31.2		231.5
3/30/2015	11:30	3	-7.3	-1.7	31.4		241.2
3/31/2015	19:31	3	-8.6	-1.7	31.9		248
4/1/2015	17:00	3	-10.6	-1.7	32.7		255.5
4/2/2015	11:43	3	-11.1	-1.7	32.2		239.5
4/3/2015	16:30	3	-10.7	-1.7	32.3		240.3
4/4/2015	12:30	3	-9.3	-1.8	32.7		244.1
4/5/2015	14:00	3	-10.1	-1.8	32.9		244.2
4/6/2015	9:30	3	-10	-1.8	33		243.4
4/8/2015	11:00	3	-11.3	-1.8	33.4		255.6
4/10/2015	18:00	3	-9.3	-1.8	34.1		270.1
4/12/2015	13:52	3	-9.7	-1.9	34.5		263.7
4/13/2015	9:21	3	-9.7	-1.8	34.5		261.5
4/14/2015	3:00	3	-9.8	-1.8	35.1		262.6
4/16/2015	13:00	3	-10.2	-1.8	35.1		261.5
3/24/2015	17:45	4		-1.6	22.1	7.5	
3/25/2015	12:00	4		-1.7	29.7	11	
3/26/2015	9:00	4	-9.2	-1.8	26	12	
3/28/2015	11:21	4	-7.6	-1.7	30.9		240.1
3/29/2015	14:31	4	-7.4	-1.7	31.2		240.9
3/30/2015	11:30	4	-7.8	-1.7	31.3		239.8
3/31/2015	19:31	4	-7.7	-1.7	31.6		238.1
4/1/2015	17:00	4	-10.5	-1.7	31.7		244.8
4/2/2015	11:43	4	-9.7	-1.7	32		244.5
4/3/2015	16:30	4	-9	-1.7	32.3		241.5
4/4/2015	12:30	4	-8.9	-1.7	32.5		243.6
4/5/2015	14:00	4	-8.9	-1.8	32.7		242.6
4/6/2015	9:30	4	-9.1	-1.8	32.8		242.3
4/8/2015	11:00	4	-9.5	-1.8	33.2		247.7
4/10/2015	18:00	4	-10	-1.9	33.9		290
4/12/2015	13:52	4	-10.4	-1.9	34.6		281.3
4/13/2015	9:21	4	-10.5	-1.9	34.7		285.2
4/14/2015	3:00	4	-10.5	-1.9	34.9		283.2
4/16/2015	13:00	4	-10.7	-1.9	35		283.6
3/24/2015	17:45	5		-1.6	26.1	8	
3/25/2015	12:00	5		-1.6	29.6	13	
3/26/2015	9:00	5	-7.8	-1.7	30.4	13	
3/28/2015	11:21	5	-7.9	-1.7	30.9		233
3/29/2015	14:31	5	-8.6	-1.7	31.2		233.9

Date	Time	Tank	Surface Temperature (˚C)	Water Temperature (˚C)	Water Salinity	Ice Thickness (cm)	2π Surface Irradiance (µmol photons m^{-2} s^{-1})
3/30/2015	11:30	5	-9.4	-1.8	31.5		230.7
3/31/2015	19:31	5	-10.4	-1.7	31.9		234.7
4/1/2015	17:00	5	-10.6	-1.7	32.1		231.1
4/2/2015	11:43	5	-10	-1.7	32.3		236.3
4/3/2015	16:30	5	-9.6	-1.8	32.7		234.5
4/4/2015	12:30	5	-9	-1.8	32.9		234.4
4/5/2015	14:00	5	-9.4	-1.8	33.1		234.1
4/6/2015	9:30	5	-10.3	-1.8	33.3		235.1
4/8/2015	11:00	5	-10.5	-1.9	34.1		232.1
4/10/2015	18:00	5	-10.4	-1.9	35.1		266
4/12/2015	13:52	5	-12	-2	35.8		270
4/13/2015	9:21	5	-11.8	-1.9	35.9		271.2
4/14/2015	3:00	5	11.9	-1.9	35.8		269.9
4/16/2015	13:00	5	-11.3	-1.9	35.9		271.4
3/24/2015	17:45	6					
3/25/2015	12:00	6		-1.6	29.8	11	
3/26/2015	9:00	6	-6.8	-1.7	30.7	12	
3/28/2015	11:21	6	-9.3	-1.9	17.8		242
3/29/2015	14:31	6	-7.5	-2.1	10.7		239.9
3/30/2015	11:30	6	-10.6	-2.2	5.9		237.7
3/31/2015	19:31	6	-9.7	-2.3			244.9
4/1/2015	17:00	6	-10.6	-2.4	4.4		246.2
4/2/2015	11:43	6	-10.6	-2.5			245.5
4/3/2015	16:30	6	-9.9	-2.6	4.4		242.5
4/4/2015	12:30	6	-9.1	-2.7	4.4		243.5
4/5/2015	14:00	6	-9.4	-2.8	4.4		243.1
4/6/2015	9:30	6	-10.9	-1.8	4.4		248.8
4/8/2015	11:00	6	-11.1	-2.6	4.6		232.5
4/10/2015	18:00	6	-10	-3.1			275.3
4/12/2015	13:52	6	-9.7	-3.1			283
4/13/2015	9:21	6	-9.8	-3.1			282.2
4/14/2015	3:00	6	-9.8	-3.1	9.7		282.3
4/16/2015	13:00	6	-10	-3.1			281.2

Appendix Table 11. Cold room monitoring data from Y2 (2015).

Date	Time	Set Point (˚C)	Room Temperature (˚C)	Air Temperature (˚C)	4π Under-Ice Irradiance (Tank 3; μmol photons m^{-2} s^{-1})
3/24/2015	17:45	-15			
3/25/2015	12:00	-15		-14.5	
3/26/2015	9:00	-15	-15	-15.4	
3/28/2015	11:21	-15	-15.2	-17.3	14.61
3/29/2015	14:31	-15	-15.3	-15.8	14.71
3/30/2015	11:30	-15	-14.9	16.5	15
3/31/2015	19:31	-15	-15.1	-13.3	3.2
4/1/2015	17:00	-15	-14.7	-16.5	2.1
4/2/2015	11:43	-15	-15.3	-15.9	2.13
4/3/2015	16:30	-15	-14.8	-15.5	2.3
4/4/2015	12:30	-15	-15.4	-16.6	1.9
4/5/2015	14:00	-15	-15.1	-16.4	-2.1
4/6/2015	9:30	-15	-15.1	-116	0
4/8/2015	11:00	-15	-14.8	-17.9	1.9
4/10/2015	18:00	-15	-14.6	-15.8	1.3
4/12/2015	13:52	-15	-15.4	-15.6	
4/13/2015	9:21	-15	-15.3	16.1	
4/14/2015	3:00	-15	-14.9	-15.2	
4/16/2015	13:00	-15	-14.4	-16.5	

The Department of the Interior Mission

As the Nation's principal conservation agency, the Department of the Interior has responsibility for most of our nationally owned public lands and natural resources. This includes fostering the sound use of our land and water resources, protecting our fish, wildlife and biological diversity; preserving the environmental and cultural values of our national parks and historical places; and providing for the enjoyment of life through outdoor recreation.The Department assesses our energy and mineral resources andworks to ensure that their development is in the best interests of all our people by encouraging stewardship and citizen participation in their care. The Department also has a major responsibility for American Indian reservation communities and for people who live in island communities.

The Bureau of Ocean Energy Management

The Bureau of Ocean Energy Management (BOEM) works to manage the exploration and development of the nation's offshore resources in a way that appropriately balances economic development, energy independence, and environmental protection through oil and gas leases, renewable energy development and environmental reviews and studies.